Assessing the effects of increased summer flooding in an impounded mangrove with the use of remote sensing

31 July 2015

Master's Thesis
Maartje Oostdijk

Sustainable Development,
Joint Master, Global Change and Ecosystems
30ECTS

Supervised by:

Maria João Santos (Utrecht University)
Sonia Silvestri (Duke University)
Jos Verhoeven (Utrecht University)

Acknowledgements

By sending an email to Sonia Silvestri, whose course in remote sensing I followed in Venice, I got to work on this thesis project. The academic world is tiny apparently because it happened that she was collaborating with a professor from Utrecht University: Jos Verhoeven. I worked on the subject which intrigues me most: coastal ecosystems, with the tool that I wanted to acquire: remote sensing analysis. I have had a great time doing fieldwork in Florida and visiting Duke University, where the research environment was very inspiring.
For the fieldwork I especially want to thank Dennis Whigham who accompanied me to the field every day, has shown great patience and has thought me a lot about the ecosystem, which does not exists of pixels, you are right on that Maria! Also Jos deserves a great thank you, because if it wasn't for him I would have never been to Florida or the US for my thesis at all. Also, Jos brought an incredibly large instrument (the Fieldspec) all the way from the Netherlands to the US for the purpose of this study. I want to thank Sonia, who was always there to answer all my questions on the pre-processing of my data. This became such a small part of the written thesis, but really it was more than half the work, apparently that is normal. Then... all the time and effort that Maria João Ferreira Santos took to help me write this thesis, I really never expected that of a supervisor. I learned so much in this process: how to outline the study, the methodological issues and then how to write it down. Honestly, Maria, thank you for every comment!
I'm super happy that there were people willing to look over my thesis when my own eyes became insensitive for the illogic parts of it thank you: Laura, Erin and Paula. Lastly I want to thank Kora in advance for helping me hand in a printed copy while having the luxury to have written the last part of the thesis in warm and beautiful Venice.
My research would not have been the same without the financial support of stipendium Bottelier and the Miquel fund.

Abstract

Mangrove impoundments on the Indian River Lagoon, Florida, were constructed as a method for mosquito control. Artificial dikes were built up around the marsh areas to keep the mangroves continuously flooded as the black salt marsh mosquito, which is common in the area, will not oviposit in standing water. By 1959 over 3,240 ha of wetlands were impounded in the Indian River Lagoon (Rey et al., 2012).
Continuous impounding is known to have negative effects on the health of mangrove vegetation. A simple change in water management: using a rotational impoundment management (RIM), was hypothesized to prevent the adverse consequences of continuous impounding, while at the same time allowing for noxious insect control. RIM involves the pumping of estuarine water into the impoundments to raise the water by 30 cm in spring and summer, the reproductive season of the black salt marsh mosquito.
With this thesis I assessed the effects of the RIM strategy in an impounded mangrove in Florida, five years after the implementation of RIM. More specifically I examined whether there have been changes in the spatial distribution and state of the dominant black mangrove vegetation on the scale of the impoundment, before and after the implementation of RIM by making use of aerial photographs and high resolution satellite data.
To follow distribution and extent of the mangrove vegetation I performed a land-cover classification with different classes of vegetation on color infrared aerial photographs from 2008 and 2010 and a Worldview-2 satellite image from 2014. In addition I created a map of leaf area index (LAI) by linear regression of vegetation indices and in situ collection of LAI to assess the current productivity of the vegetation on the scale of the mangrove impoundment.
I found that an increase in mangrove vegetation took place after implementation of RIM in the mangrove impoundment and that the productivity of the vegetation measured by NDVI increased by 8% over the whole impoundment. The greatest shifts took place in areas without vegetation cover or with stunted mangrove vegetation, associated with hypersaline conditions. Productivity measured by NDVI in those regions increased on average by more than twofold. The succession towards denser classes of vegetation at the hypersaline interior indicated that re-establishment of mangrove vegetation took place.
However, I found that current productivity over the whole impoundment, years after implementation of RIM, nonetheless remained lower than that of mangrove vegetation that was not impounded.

Contents

Universiteit Utrecht

List of abbreviations

DM = Digital Mapping camera

ENVI = Environment for Visualizing Images

GPS = Global Positioning System

LAI = Leaf Area Index

MODIS = Moderate-resolution Imaging Spectroradiometer

MSAVI = Modified Soil Adjusted Vegetation Index

NDVI = Normalized Difference Vegetation Index

NIR = Near Infrared

PAR= Photosynthetic Active Radiation

RIM = Rotational Impoundment Management

ROI = Region of Interest

SR = Simple Ratio

UCX = UltracamX

VI = Vegetation Index

WV2 = Worldview 2 satellite

1. Introduction

Mangrove ecosystems cover up to 75% of tropical and subtropical shorelines and occur between a latitude of 25-30°S up to 25-30°N (Tomlinson, 1986). Mangroves are important ecosystems for coastal protection and they offer habitat and hatching areas for many important marine species. The trees stabilize the shoreline with their root system, preventing erosion and acting as "bioshields" against destructive impacts from storms or storm surges (Vogt et al., 2012).

Species composition and structure of mangrove ecosystems depend on physiological tolerances and competitive interactions (Tomlinson, 1986). Mangrove ecosystems are highly sensitive to changes in frequency and duration of tidal inundation, salinity and composition of the soil and changes in water quality (Kuenzer et al., 2011). Hydrology is therefore a main factor determining the stability of mangrove ecosystems (Vogt et al. 2012). Mangroves are diminishing worldwide due to sea level rise as well as destruction of habitat for fish culture. Moreover, management strategies such as continuous impounding can have damaging effects on vegetation and water quality (Rey et al., 2012).

1.1.1. History of the Impoundments

The impoundments on the Indian River Lagoon, Florida, were constructed as a method for mosquito control. Since the black salt marsh mosquito (*Aedes taeniorhynchus),* that is common in the area, will not oviposit in standing water, flooding of the area is an effective method for mosquito control. For the construction of the impoundments artificial dikes were built up around the marsh areas; these areas were initially kept permanently flooded. In 1930 impounding mangroves was discovered to be an effective means of mosquito control, and by 1959 over 3,240 ha of wetlands were impounded in the Indian River Lagoon (Rey et al., 2012).

Impounding wetlands has negative impacts on vegetation, fish communities and water quality (Brockmeyer et al., 1996). Transient estuarine fish species could no longer access the impoundments for nursery or feeding purposes (Rey et al., 2012). The impacts of impounding on the vegetation were severe. For example, halophyte species such as saltwort (*Batis maritime*), glasswort (*Salicornia virginica*) and dwarf glasswort (*Salicornia bifelovii*) disappeared from the marshes. In some areas black mangroves (*Avicennia germinans*) were eliminated (Brockmeyer et al., 1996) as black mangroves do not tolerate submersion for a long period of time. Red mangroves (*Rhizophora mangle*) can better withstand submersion and in some areas a diverse mangrove or marsh vegetation was replaced by almost monospecific stands of red mangrove (Rey et al., 1990).

Since the early 1960's there has been an effort to rehabilitate the mangroves and thus to reconnect the impoundments to the Indian River Lagoon (Brockmeyer et al., 1996). Rehabilitation with the use of culverts or rotational impoundment management (RIM) were chosen as suitable methods. Rehabilitation through culverts allows exchange of water with the lagoon and results in re-establishment of the original vegetation as well as in a diversity of fish species and decapods (Rey et al., 2012).

Even after reconnecting the impoundments to the Indian River Lagoon, mangrove vegetation inside impoundments shows a zonation that is distinct from the zonation that is found in pristine mangrove ecosystems. Feller at al. (2003) compared zonation in a reconnected impounded mangrove on the east coast of Florida to a pristine ecosystem in in Belize. In both mangrove ecosystems, the pristine and the impounded, a height gradient was found with taller trees on the exterior and dwarf trees on the interior

(Feller et al., 2003). In the pristine ecosystem red mangrove was the dominant species, exhibiting a height gradient from fringe to interior, with higher trees on the fringe and mangroves with stunted growth on the interior. In the impounded mangrove species dominance shifted from fringe to interior, with dominantly red mangrove on the fringes where salinity is lower and dominantly black mangrove on the interior (Stringer et al., 2010). The impounded mangrove in Florida was hypersaline on the interior, caused by high levels of evaporation and the isolation from the tidal circulation (Feller et al., 2003). Black mangrove is dominant where salinity conditions approach those of seawater, as black mangrove tolerates high salinity conditions better than red mangrove, however, growth of black mangroves is stunted and limited under hypersaline conditions (Verhoeven et al., 2014).

1.1.2. RIM and its effects on the mangrove ecosystem

RIM is a method that allows the water level in the impoundment to be raised by 30 centimeters in the reproductive season of the mosquitos in spring and summer and therefore reduces their reproductive output (Verhoeven et al., 2014). In comparison with the open estuary with culverts, RIM is a significantly more effective method to reduce mosquito proliferation (Floore, 2006).

Impounding mangrove areas or using RIM to temporarily flood an area are expected to have large influences on the primary production as well as species composition (Stringer et al., 2010). This is due to the fact that coastal mangroves are largely controlled either directly or indirectly by hydrology: salinity and water levels control plant community composition, whereas primary production is mainly controlled by nutrients (Stringer et al., 2010). Marchand et al. (2004) found for example that red mangroves grow in places subjected to the greatest variability in freshwater influxes, suggesting that red mangrove withstands occasional inundation by freshwater better than black mangrove. Rey et al. (1990) found that the summer flooding inhibits primary production during the summer season compared with non-impounded mangroves. However, during the summer season primary production is low in the region due to high temperatures and high intertidal salinities, thus effects on the primary production over the whole year are different as will be discussed below. The study also found that litter has a longer residence time in the impounded marshes, resulting in a nutrient reservoir (Rey et al., 1990, Rey et al., 2012) which is possibly beneficial for primary production as the mangroves in the impoundments are nitrogen limited (Feller et al., 2003). Moreover, with the pumping of estuarine water into the impoundments nutrients are added to the mangrove ecosystem (Verhoeven et al., 2014).

Implementation of RIM has been found to result in decreased nitrification and denitrification, increased nitrogen contents in the mangrove leaves and increased shoot growth and leaf production of black mangrove (Verhoeven et al., 2014). In addition, pore water salinity had decreased on average by 43% as a result of RIM (Laanbroek et al., 2012), which was most likely the reason for increased leaf production in the zones with dwarf or sparse black mangrove vegetation (Verhoeven et al., 2014). In contrast with the findings of Rey et al. (1990) Verhoeven et al. (2014) thus found an increase in primary production of, in this case specifically black mangrove, over the year when before and after implementation of RIM were compared. This was mainly due to the moderating effect on salinity levels of pumping lagoon water into the mangrove impoundment (Verhoeven et al., 2014).

1.2. Remote sensing of mangroves

Remote sensing has been successfully applied to extrapolate local field observations to landscape level effects in mangrove areas (Rey et al. 2009). Mangrove areas are difficult to access and field campaigns are costly and time intensive. Remote sensing in combination with field measurements can reduce these costs (Rey et al. 2009).
Several types of remote sensing data such as aerial photographs have previously been used to classify and map mangrove forest and assess changes in coastal ecosystems (Kuenzer et al., 2011, Krause et al., 2004; Geneletti and Gorte, 2003). For example, Rodrigues and Feller (2004) mapped mangrove forest deforestation on the Twin Cays Archipelago, Belize, with the use of black and white aerial photography in combination with multispectral high spatial resolution IKONOS imagery. Krause et al. (2004) established a classification distinguishing red and black mangrove species in North Brazil using color aerial photography.
Spatial and spectral characteristics are used to study and monitor mangrove areas. Well established indices such as the normalized difference vegetation index (NDVI) or the normalized difference water index (NDWI), obtained from satellite data or airborne sensors, can indicate changes in leaf area index (LAI), biomass and photosynthetic activity or canopy water content, respectively (Huete et al., 2014). Most recent studies make use of high spatial resolution imagery from satellites such as Worldview 2 and GeoEye-1 (Chavez, 2014) to assess mangrove productivity (Heumann, 2011a). Recent advances in the use of radar imagery make it possible to obtain more accurate estimations of mangrove biomass (Heumann, 2011b). In addition the use of hyperspectral imagery increases the possible applications of remote sensing by providing fine spectral resolution data that can be used to detect subtle differences in spectral reflectance (Heumann, 2011b).
Recent papers have been published using high-resolution imagery from sensors such as WV2, Quickbird and IKONOS to: determine spatial distribution and current state (Rodrigues and Feller, 2004); discriminate species and estimate biomass as well as assess vegetation indices in relation to LAI (Kovacs et al., 2009) and to detect change in mangrove ecosystems (Lee and Yeh, 2009). LAI of plant canopies is an important structural parameter that controls photosynthesis, carbon and nutrient cycle and energy, gas carbon and water exchanges in ecosystems (Pu and Cheng, 2015). LAI is therefore one of the biophysical parameters that are widely used to monitor forest stands. Kovacs et al. (2009) used high spatial resolution remote sensing (IKONOS and Quickbird) in combination with in situ LAI measurements to assess the condition of a mangrove forest of the Mexican Pacific. It was found that a large part of the mangrove forest was experiencing a considerable state of degradation.
Not much published research exists that assesses the effects of impoundments on mangrove vegetation with the use of remote sensing. Vogt et al. (2012) studied the role of impoundment and forest structure on the resistance and resilience of mangrove forests to hurricanes. The recovery from hurricane damage was investigated at three impounded mangrove areas along the Indian River Lagoon which all had RIM implemented. Silvestri et al. (2014) created time series of MODIS and Landsat NDVI of the two adjacent impoundments along the Indian River Lagoon that were investigated previously by Verhoeven et al. (2014). No clear difference was found between the impoundment with RIM and the reference impoundment before and after RIM. The branch length increment, increased leaf production and increased nitrogen content found in the field by Verhoeven et al. (2014) were thus not supported by the NDVI

values obtained from Landsat (30m spatial resolution) and MODIS (250m spatial resolution) remote sensing imagery.

1.3. Research aim

With this study I aim to assess the effects of a hydrological change in two impounded mangroves on the east coast of Florida, along the Indian River Lagoon. The objective of the project is to investigate whether differences in water management have consequences for the productivity and composition of the mangrove vegetation. In one of the two impoundments studied the rotational impoundment management (RIM) strategy was implemented in the year 2009 as a method for noxious insect control. Verhoeven et al. (2014) showed that implementation of RIM was beneficial overall for the growth of the black mangrove vegetation (i.e. increased branch length and increased leaf production were found for dwarf and sparse mangrove). However, up to the present it has been difficult to assess the change in productivity and distribution of mangrove vegetation on the scale of the impoundment. Silvestri et al. (2014) found no clear difference in productivity of the mangrove vegetation between before and after implementation of RIM with the use of low spatial resolution remote sensing imagery (30 and 250 m) For this reason I will use high spatial resolution remote sensing in this study to assess the effects of RIM on the impounded mangrove ecosystem on the Indian River Lagoon.

1.4. Research questions

To obtain information on the condition of vegetation on the scale of the impoundment I posed the following research question: *Does the implementation of rotational impoundment management (RIM) influence the extent, composition and productivity of the mangrove vegetation in an impounded mangrove area in Florida at the impoundment scale?*

I divided this question into the following sub-questions:

A. *Has the mangrove distribution and species composition changed with RIM?*
B. Is there a change in productivity of the vegetation before and after the implementation of RIM?
C. What is the current state of mangrove vegetation on the scale of the impoundment?

1.5. Hypotheses

Based on the previous field results I hypothesize that the RIM strategy has a positive effect on the productivity (in the form of leaf production and shoot growth) of the mangrove vegetation and I therefore expect an increase in productivity of the vegetation. Moreover, I expect an increase in extent of vegetation (black mangrove and herbaceous vegetation) which before RIM were associated with salt pans or dwarf black mangrove vegetation.

A. *Implementation of RIM will result likely result in higher abundance of dense black mangrove and reduction of sparse black mangrove.*
B. RIM will likely result in an increase in productivity (Verhoeven et al., 2014).
C. The spectral indices relate linearly to field measurements of LAI (Kovacs et al., 2005; Kovacs et al., 2009), therefore the remote sensing indices can be used to extend the scale of field measurements of productivity of the mangrove ecosystem (Lee and Yeh, 2009). The impounded mangrove is nonetheless expected to have a lower productivity of vegetation in the hinterland compared to the fringe (Feller et al., 2003).

2. Methodology

2.1. Study area

The study was conducted in two impoundments located at N27˚330, W80˚330 on the east side of the Indian River Lagoon between Vero Beach and Fort Pierce, Florida.
Meteorological data of the area from the last 15 years can be found in Appendix 1.
In Table 1 an overview of the management history in both impoundments is presented. In the initial stage of both impoundments the dikes did not contain culverts and both areas were isolated from tidal circulation. In the year 1979 the dike in impoundment 23 was breached (Verhoeven et al., 2014), water levels in impoundment 23 were then largely controlled by tidal circulation. In later years culverts were implemented in impoundment 24, however tidal exchange was still limited because the culverts were small in size and number (Verhoeven et al., 2014).
In March 2009 pumping began in Impoundment 24 and from that year on it is annually flooded between March and September. Water is pumped in and drains back to the Indian River Lagoon through the open culverts (Verhoeven et al., 2014).

Table 1. Management history of the two impoundments (Verhoeven et al., 2014)

Event	Reference impoundment (23)	Impoundment with RIM (24)
Closing of the dike	1966	1970
Dike breach	1974	
Placement of one culvert		1985
Placement of four additional culverts		1987
Implementation rotational impoundment management		Early spring 2009

Vegetation in both impoundments is dominated by black mangrove. Red mangrove is abundant and dominant near the fringe of the Impoundments. White mangrove (*Laguncularia racemosa*) and buttonbush (*Conocarpus erectus*) are also present and typically occur on higher elevation locations within the impoundments and at the wetland-upland border (Feller et al., 2003). Black mangrove tends to be dense near open-water areas and sparse near the interior where dwarf black mangroves are found (Feller et al., 2003).

Impoundment 23 (Table1) was used as a control by Verhoeven et al. (2014) and for the present study. Throughout the rest of the paper I address impoundment 23 as the impoundment without RIM (no RIM). In this study I used a second control area which is located outside the impoundments; I refer to this area as 'non-impounded'. This area was needed for the present study because of two reasons: first the impoundment without RIM was not captured on the imagery of 2008 therefore no before and after comparison could be made using this impoundment; second it is informative to compare the state of the vegetation inside the impoundments to a non-impounded area. The respective sizes of the areas (Figure 1) used in this study are as follows: (1) the non-impounded area is 170544 m^2, (2) the impoundment with RIM is 248900 m^2, and (3) the impoundment without RIM is 617318 m^2.

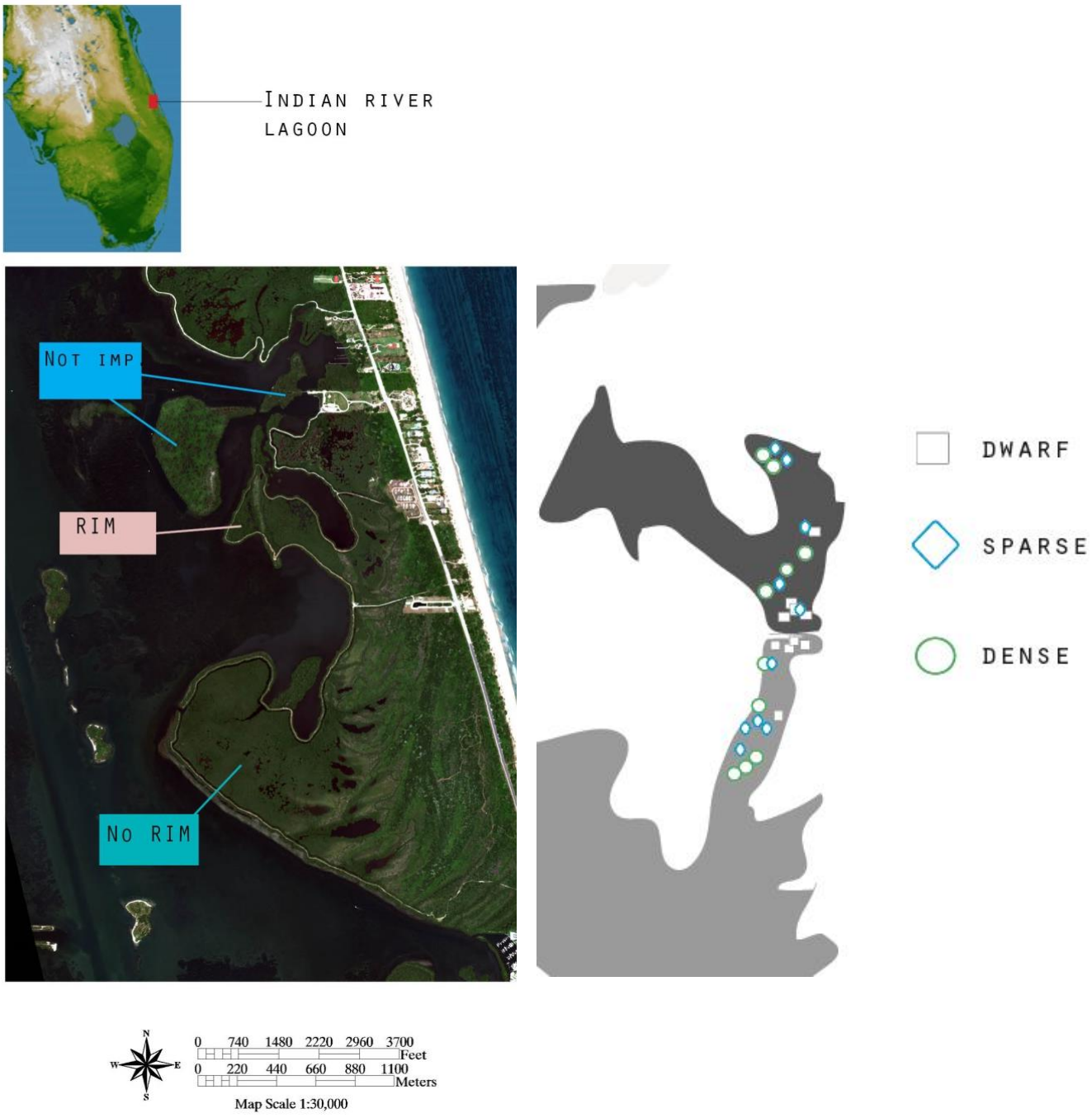

Figure 1. (left) RIM - Impoundment 24 (upper) and no RIM - Impoundment 23 (lower) on the WV2 image (RGB). The impoundments are located N27.330, W-80.330 on the east side of the Indian River Lagoon on North Hutchinson Island between Vero Beach and Fort Pierce, Florida. The non-impounded area, the impoundment with RIM and the impoundment without RIM are pointed out. (right) The dwarf, sparse and dense sites in both impoundments.

Verhoeven et al. (2014) selected five replicate locations of three different black mangrove cover types in the impoundment with and in the impoundment without RIM. For each replicate location 5 plots of 2 by 2 meter with a black mangrove cover type were selected. The characteristics of the cover types are listed in Table 2. The choice of cover types was based on the zonation of mangrove vegetation inside the impoundments (Feller et al., 2003). Dwarf black mangrove zones are located in the hinterland and are associated with salt pans where there is either no vegetation, or scattered vegetation composed of individuals or patches of black mangrove often in combination with saltwort, Virginia glasswort, and dwarf glasswort (Feller et al. 2003). The intermediate zone is located between the fringe with high stands of red mangrove and the hinterland with dwarf mangrove (Feller et al., 2003). The intermediate zone contains dense and sparse zones of black mangrove vegetation.
For the present study I extended the size of the five replicate locations selected by Verhoeven et al. (2014) inside the different zones to a size of on average 130 m^2 per site, as one of the aims of the present study was to extend the scale of the local field results. The black mangrove vegetation at these selected sites in the dwarf, sparse and dense zones is mainly characterized by the cover types described by Verhoeven et al. (2014).

Table 2. Criteria for replicate location selection (Verhoeven et al. 2014)

	Proportional cover	**Tree height**
Dwarf cover	30% cover of mangrove	Up to 1 meter
Sparse cover	30-80% cover of mangrove	1 to 3 meter
Dense cover	80-100% cover of mangrove	Greater than 3 meter

2.2. Remote sensing data and pre-processing

For the present study I used high spatial resolution color infrared aerial photography and a Worldview-2 (WV2) satellite image to assess the distribution, composition and state of the mangrove vegetation. I mapped the distribution of mangrove vegetation to see if succession is taking place with the use of the color infrared aerial photography. Moreover, I produced a map of leaf area index to assess current productivity of the vegetation. I constructed this map by calculating vegetation indices using the WV2 image and I then related these vegetation indices (also related to productivity of vegetation) to in situ obtained LAI. A field campaign served to collect LAI measurements of several locations in the impoundments, and to record the locations of the different species using GPS measurements.

2.2.1. Remote sensing data

Table 3 shows the specifications as well as the different spectral resolutions of the sensor types I used for the purpose of this study. As can be observed all sensor types provide imagery with a very high spatial resolution. The WV2 sensor has a narrower bandwidth than the orthophotographs (as can be seen in Table 3). To obtain the at-surface-reflectance that can be used for further analysis I performed several steps of preprocessing. These steps included geo-rectification, atmospheric correction and pan-sharpening. These steps are described in the following paragraphs.

Table 3. Spatial resolution, collection date and spectral resolution of the images used for Digital Mapping camera (Intergraph, 2009) and UtracamX (Christopherson, 2010) and WV2 (Updike, 2010).

Sensor	***Satellite: WV2 multispectral***	***Satellite: WV2 panchromatic***	***Airborne: UltracamX***	***Airborne: Digital Mapping camera***
Collection date	10-06-2014	10-06-2014	03-12-2010	22-04-2008
Spatial resolution	2 m	0.5 m	0.15 m	0.30 m
Color	***Wavelength (nm)***			
Blue coastal	400–450 nm			
Blue	450–510 nm		410-540 nm	400-580 nm
Green	510–580 nm		490-660 nm	500-650 nm
Yellow	585–625 nm			
Red	630–690 nm		590-700 nm	590-675 nm
Red Edge	705–745 nm			
NIR	770–895 nm		690- 980 nm	675-850 nm
NIR2	860–1040 nm			
Panchromatic		450–800 nm		

As can be seen in Figure 2, WV2 spectral response curves and those of the Ultracam X are very different. The bandwidths of the WV2 spectral bands are narrower as pointed out by Heendenka et al (2010) in comparison to those of the airborne data. For example the red band in the WV2 image (630–690 nm) will give a lower reflectance for plant species than the UltracamX red band (590-700nm) as absorption due to photosynthetic activity is strongest around 640-660 nm (Kumar et al, 2001). In addition reflectance in the NIR1 (770–895 nm) and NIR2 (860-1040nm) bands of the WV2 image will be higher because of reflectance from leaves (due to their physiological structure) and is the highest in the range 760-1100 nm (Kumar et al., 2001). As can be seen in Figure 2a the Ultracam spectral response curve shows the strongest spectral response between 700-760 nm in the NIR band which is very different from WV2 sensor (highest sensitivity around 770: Figure 2b). This is likely to affect the results from each sensor, and therefore I made no direct comparisons between the two imagery datasets.

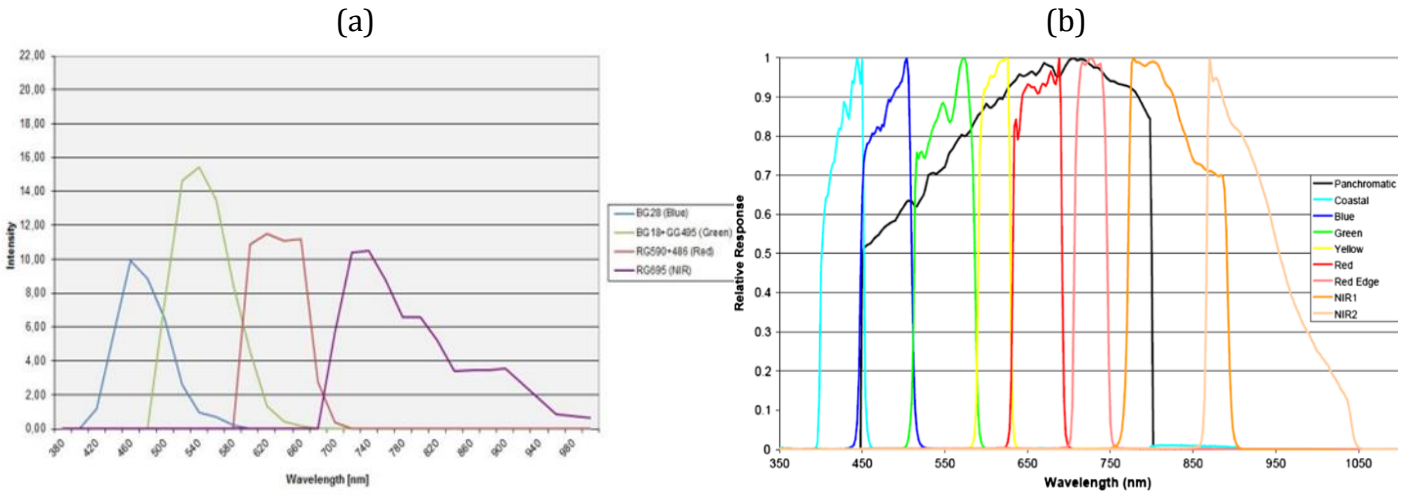

Figure 2. (a) Spectral response curves of the WV2 multispectral and panchromatic sensor (Christopherson, 2010). (b) Spectral response curves of the Ultracam-X multispectral sensor (Updike, 2010).

2.2.2. Geometric correction

The aerial photographs (DM and UCX) were orthorectified by Aerial Cartographics of America (Orlando, Florida). For geometric correction of the aerial photography, 394 ground control points were used on a mosaic of 84 images (Humphrey, 2011).
I registered the WV2 multispectral image and panchromatic image using image to image registration in ENVI 4.7 software (Exelis Inc, Virginia, USA), using the 2010 orthophotograph as a base image. I used 21 ground control points for geometric correction of the WV2 satellite imagery that I selected by visual identification on the aerial photographs using objects with a clearly distinguished geometry such as the roof of a house or the corner of a pier. To assess the accuracy of the geometric correction I used the root mean square error (RMSE), which measures the positional difference between the two images; this value should be as low as possible and a value lower than one (pixel) is considered excellent (Jacobsen, 2003). Geometric correction of the multispectral imagery achieved a sub-pixel spatial accuracy (RMSE = 0.37). I then used the same number of ground control points to register the panchromatic band, again achieving sub pixel accuracy (RMSE=0.5). The algorithm that I used to warp the June files to match the orthophotograph of 2010 was the nearest neighbor algorithm. The nearest neighbor algorithm is computationally efficient and delivers results comparable to more complex algorithms (Chen et al., 2003). The orthophotographs of 2008 and 2010 showed good spatial agreement (RMSE=0.42).

2.2.3. Atmospheric and radiometric correction

To correct for additive path radiance I applied a dark pixel subtraction to the orthophotographs in ENVI 4.7 software (Heenkenda et al., 2014). By employing the empirical line method, with the field obtained reflectance values of pseudo-invariant targets, I converted the digital numbers of the aerial photographs (2008 and 2010) to reflectance values. The empirical line is a known method for radiometric correction of remote sensing imagery (Honkavaara et al., 2009). The calibration lines as well as validation plots for the method can be found in Appendix 2.

To convert the digital numbers of the WV2 image to at-sensor radiance, I used the gain values found in the metadata. Then I corrected the multispectral image atmospherically in Envi5.2 using the FLAASH application that runs the MODTRAN5 radiative transfer model (Manakos et al., 2011). The panchromatic band could not be atmospherically corrected using FLAASH as the file needs to contain multiple bands, and thus I applied the empirical line method to convert the pan-band at-sensor radiance to at-surface reflectance (Pu & Landry, 2012). The empirical line and the function that I applied to the panchromatic band can be found in Appendix 2.

2.2.4. Pan-sharpening

To obtain a higher resolution image I performed a pan-sharpening procedure on the WV2 image. This was needed in order to create an image of comparable spatial resolution as the aerial photographs as well as to obtain more accurate classification results (Heenkenda et al, 2014; Pu & Landry, 2012).

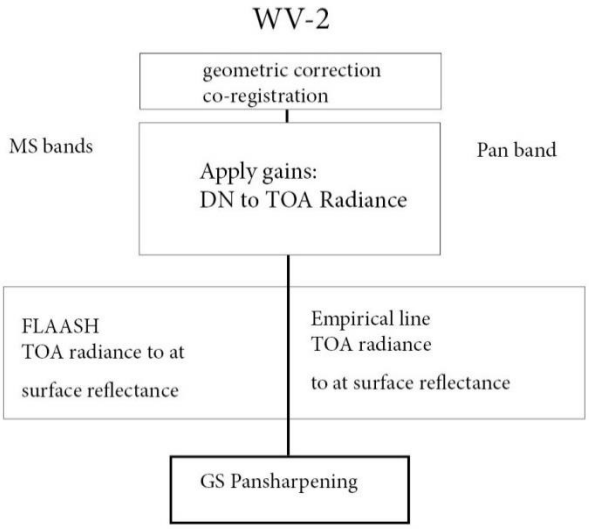

Figure 3. The steps of preprocessing that were followed to obtain the pan-sharpened WV2 image.

Figure 3 shows the steps that I followed to create the Pan-sharpened WV2 image. I created a pan-sharpened WV2 image by fusing the 2m resolution multispectral bands with the 0.5m resolution panchromatic band. I performed the pan-sharpening with the use of the Graham Smith (GS) algorithm, as in previous studies this resulted in the least distortion in WV2 imagery from all the algorithms available in ENVI software (Padwick et al., 2010). The GS algorithm has shown especially better performance in forested areas (Padwick et al., 2010). From all land cover types (for example urban, desert, coast, rocks) tested by Padwick et al. (2010) the forest was the most similar to the mangrove ecosystem in the present study.

2.3. Field sampling

2.3.1. Field collection of spectra

During the field campaign the first two weeks of March 2015 I collected field spectra of pseudo-invariant targets with an ASD Fieldspec Pro (350-2500 nm, output: each nm) that measured true reflectance in the field. I selected several pseudo-invariant targets

for each photography and included dark and bright targets. The pseudo invariant targets included: the concrete pier in the Marina, the gravel of a dirt road, the brick road on an abandoned terrain, the water surface in the marina, the water surface of a pond, dark and light asphalt. For each target I averaged five measurements of the ASD Fieldspec Pro (ASDinc, 2002). Due to a lack of time and a failed connection between the laptop and the ASD Fieldspec I did not collect spectra of vegetation.

2.3.2. In situ collection of leaf area index

LAI is a good field level surrogate for plant productivity and it can be linked with imagery derived LAI metrics or other vegetation indices (Pu and Cheng, 2015).
I measured the leaf area index of 161 locations inside the impoundments using a portable AccuPAR LP-80. The AccuPAR has been shown to give more accurate estimations of LAI then the more commonly used LAI 2000 (Facchi et al., 2010; Wilhelm et al., 2000).
The AccuPAR measures incoming radiation in the photosynthetic range (400-700nm). For densely vegetated areas a Photosynthetic Active Radiation (PAR) meter and data logger were implemented on the dike around the impoundment. The datalogger logged one above canopy PAR measurement every 30 seconds. For each above canopy PAR measurement, I averaged 10 below canopy PAR measurements. When the measurements of the AccuPAR were uploaded on the computer, I matched the timestamps of the PAR measurements of the data logger and AccuPAR and subsequently post-processed the data in a spreadsheet provided by Decagon Devices. I performed the LAI measurements on 10 sunny days the first two weeks of March, the two hours before and after solar noon.

AccuPAR LP-80 uses the following equation to determine LAI (Decagon Devices, 2013):

$$L = \frac{\left[\left(1 - \frac{1}{2K}\right) fb - 1\right] ln\tau}{A(1 - 0.47fb)}$$

In which:
L = Leaf area index
K = extinction coefficient of light in the canopy
τ = the ratio between above and below canopy measurements
$A = 0{,}283 + 0{,}785a + 0{,}159a^2$
a = the leaf absorptivity in the PAR band (AccuPAR assumes 0.9 in LAI sampling routines)
Fb= Fractional beam radiation, the ratio of direct beam radiation coming from the sun to radiation coming from all ambient sources like the atmosphere or reflected from other surfaces.

LAI is a unitless measure of the amount of cover. If LAI is determined to be 2.4 for example this means that the area sampled is covered by the equivalent of 2.4 layers of leaves (Decagon Devices, 2013).

2.3.3. GPS locations of species

I recorded locations of mangrove and mangrove associate species (N=214) using a GPS device (Garmin gpsmap 78). Mangrove species that I recorded consisted of: black mangrove, red mangrove, white mangrove and buttonbush, as well as the following mangrove associate species: saltwort and Virginia glasswort which always co-occurred. I recorded the GPS locations of the 15 (dwarf, sparse, dense) sites inside both impoundments. The spatial accuracy for all mentioned field samples (including LAI and

field spectra) was mostly within two meters, except for denser canopies in which error exceeded 2 meters. I noted distance to landscape features (for example dikes, ditch and upland forest) as well as the fraction cover of a site and the tree height.

2.4. Data analysis

2.4.1. Distribution and extent of mangrove vegetation

2.4.1.1. land-cover classification

In order to map and capture possible changes in mangrove vegetation distribution and extent (i.e. succession towards denser classes of black mangrove vegetation) I established land-cover classifications for the images of 2008, 2010 and 2014. I aimed to distinguish the classes that were determined in the field by Verhoeven et al. (2014), which were all related to height and density of the black mangrove vegetation. I modified the definitions of the classes slightly for the use of the classes in the remote sensing imagery. In Table 4 the definition of the classes for the remote sensing imagery can be found, including one class for bare soil and herbaceous vegetation and three categories for different heights/sizes of black mangrove vegetation: dwarf, sparse, dense.

Table 4. Definition of classes

Class in image	Definition 2014	2008-2010
Soil	bare soil	
Herbaceous	herbaceous vegetation such as glasswort and saltwort	
Dwarf	Trees up to 1 meter high	Canopy up to 1.5m^2
Sparse	Trees 1 to 3 meter high	Canopy 1.5m^2 to 4m^2
Dense	Trees larger than 3 meter high	Canopy larger than 4m^2

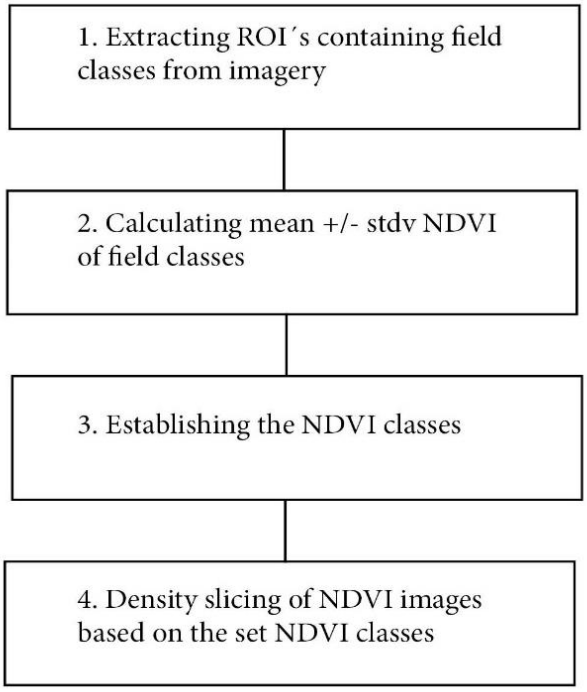

Figure 4. Flowchart showing the steps that I followed to obtain land-cover classifications from the remote sensing imagery

Figure 4 shows the steps that I followed to create land-cover classification for 2008, 2010 and 2014. During the field campaign I collected GPS data for the 15 sites at the dwarf, sparse and dense zones (Figure 1). However, no GPS data was available for single trees for the imagery of 2008 and 2010. Since the aerial photographs are of such high spatial resolution, visual identification of single trees was possible. I did this by targeting canopies of trees and larger areas of bare soil and herbaceous vegetation using the region of interest function in ENVI 4.7. Because no data on heights of the visually

selected trees were available, I based the classes on the surface area of the tree canopy (Table 4). I selected dwarf trees in the zones defined as dwarf zones (Feller et al., 2003) and the surface area of these trees was not larger than 1.5 m^2. The trees I selected for the sparse class had a surface area ranging between 1.5m^2 and 4 m^2 and I selected these trees in the sparse zones (Verhoeven et al., 2014). I selected dense mangrove trees in areas with full mangrove cover at the zones that were defined as dense (Verhoeven et al., 2014), the selected dense mangrove trees had a canopy that exceeded 4 m^2.

For the image of 2014, I used 70 ground truth samples to establish the classes and another 119 ground truth samples to test for the accuracy of the classification. Field samples were distributed across the classes, with 26 samples belonging to dwarf class, 36 to the sparse class and 31 to the dense class. Table 5 shows the amount ROI's that were used for each class for each year, each ROI contains several pixels (corresponding to at least 2 m^2, the size of the ground truth GPS data of 2015).

Table 5. Regions of interest used for the classification accuracy assessment

Year	**2008**	**2010**	**2014**
Sensor	**DM**	**UCX**	**WV2**
Soil	50	51	12
Herbaceous	50	54	14
Dwarf	50	57	26
Sparse	50	50	36
Dense	51	53	31

I then calculated NDVI (Lehmann et al., 2015*;* Lee and Yeh, 2009; Hansen and Schjoerring, 2003) for each of the images.

$$NDVI = \frac{NIR - Red}{NIR + Red}$$

NIR is the reflectance in the near infrared region (760-1100 nm), and red is the reflectance in the red region of the color spectrum (640-660 nm). In healthy vegetation red wavelengths will be absorbed by chlorophyll, as the absorbed energy is used for photosynthesis. Reflectance in the near infrared is high for vegetation because this wavelength is not used for photosynthesis, and interacts with the cell structure of leaves from which they are reflected (Myneni and Williams, 1994). NDVI is a normalized index, with values from -1 to 1. Significant linear relations between NDVI and leaf area index have been shown in mangrove forests (Heumann, 2011b; Green et al. 1997) indicating a relation between the productivity of vegetation and NDVI. NDVI values have been shown to relate to plant structure and photosynthetic activity (Myneni and Williams, 1994) as well as to aboveground biomass in mangrove ecosystems (Hirata et al., 2013). In addition Johnston and Barson (1993) found that vegetation indices related to biomass and productivity can be just as effective as more complicated statistical relationships between reflectance values to produce vegetation classifications and vegetation maps in wetlands. For the WV2 image the NIR1 band was used as it overlaps spectrally with the NDVI of the aerial photographs, which is not true for the NDVI2 band (Table 3).
To create categories of NDVI values for the classes I calculated the means and standard deviations of NDVI values of the field classes selected from the imagery (2008 and 2010)

or from ground truth data (2014) (Table 4 and 5). I then used the confidence interval (mean +/- standard deviation) to set the limits of the classes of NDVI values. With the use of density slicing in ENVI 4.7 software. I then applied these limits to the NDVI images of 2008, 2010 and 2014 to create the land-cover classifications for each of these years.

2.4.1.2. Other classification types

To be able to compare the results with other published studies, I applied a maximum likelihood classifier to the WV2 pan-sharpened image in ENVI 4.7. I did this because density slicing of NDVI values is not the most established method to map and classify mangrove ecosystems (Ozesmi and Bauer, 2002). Maximum likelihood is an established supervised classification technique for mapping wetlands. In general a maximum likelihood classification gives better results than other supervised techniques such as minimum distance to means or parallelepiped classifiers as covariance data is taken into account (Ozesmi and Bauer, 2002). Lee and Yeh (2009) carried out a maximum likelihood classification on Quickbird imagery and arrived at a high accuracy (97% and 89%) in discriminating mangrove and non-mangrove vegetation.
Due to time constraints I made no classification making use of additional spatial information. Using image segmentation and characteristics of classes beyond solely spectral information can increase classification accuracy of mangrove forest. Heenkenda et al. (2014) were able to distinguish different mangrove species in a mangrove ecosystem in Australia using object based image analysis (OBIA) in combination with a support vector machine (SVM), with an 89% accuracy. However, Heumann (2011c) classification accuracy was 29% and 25% for black mangrove and buttonwood respectively, using the same approach to mapping mangrove species in the Galapagos. Preliminary attempts for image segmentation of the aerial photographs in the present study delivered poor results and I did not pursue this further.

2.4.1.3. Proportional cover

I calculated proportional cover of the different classes for the different sites, as well as over the whole impoundment. I defined proportional cover as the proportion of pixels found for one class compared to the total amount of pixels that are contained at a site. Proportional cover served to detect the distribution and extent of mangrove vegetation and possible changes therein.
Because the images are of different spatial resolutions, proportional cover of the different classes was the most appropriate to describe the data, as any resampling algorithms are known to influence classification results (Chen et al., 2003). I calculated proportional cover for each class for each site. For each dwarf, sparse, and dense sites there were 5 replicates. I then averaged and compared results for the 5 dwarf, sparse and dense locations. In addition I calculated proportional cover for the whole RIM area; impoundment 24 (2008, 2010, 2014), no-RIM area; impoundment 23 (2010, 2014) and the non-impounded area (2008, 2010, 2014).

2.4.1.4. Change detection

To see whether and how succession takes place, I applied a change detection for the imagery of the years 2008 and 2010 using ENVI 4.7. Shifts towards higher or lower density classes provide information on the effects of RIM on the extent of mangrove vegetation. To allow for direct comparison I resampled the data of 2010 to the 0.3m resolution to match the resolution of the image of 2008.

2.4.2. Productivity

2.4.2.1. Changes in productivity (2008-2010)

To assess whether vegetation productivity (i.e. in the form of photosynthetic activity, leaf production and shoot growth) is influenced by the RIM strategy at the impoundment scale, I used a vegetation index that yields information about the productivity of the vegetation and its condition. Remotely sensed vegetation indices allow us to find out whether the hydrological change influences the state of the vegetation (Heumann, 2011a). To see whether the different sites (dwarf, sparse and dense) have responded differently to the change in water management, I calculated NDVI for all 15 sites inside the impoundment with RIM. I used field site coordinates to create regions of interest for the imagery in ENVI 4.7. In addition to this, I selected control sites in the non-impounded area. For the selection of control sites I made use of the random pixel selection tool in ENVI 4.7. I calculated NDVI for the RIM impoundment (Impoundment 24) and for the control not-impounded area.

2.4.2.2. Leaf area – canopy density

To assess whether there is a relation between the WV2 image data and in-situ leaf area index I tested several vegetation indices against field obtained leaf area index. LAI is one of the biophysical parameters that are widely used to monitor forest stands as it has been shown to relate to productivity of vegetation (canopy density; photosynthetic activity, nutrient and carbon cycle, growth) (Pu and Cheng, 2015; Kovacs et al., 2009). Using the in situ obtained leaf area index together with the remote sensing data local field data of productivity can then be extended to a larger scale (Rey et al., 2009), one of the aims of the present study. There was a time period of 9 months between the collection of in situ LAI (March 2015) and the collection date of the WV2 image (June 2014), in which changes will have taken place in the mangrove vegetation. Due to budgetary restraints no recent image could be purchased.
Little research is published relating spectral indices from WV2 imagery to in situ LAI (Pu and Cheng, 2015); i.e. testing whether WV2 imagery can be used to assess this parameter of vegetation productivity on a larger scale. For this reason I tested several indices. I selected indices on the basis of previous studies showing significant relationships between high spatial resolution satellite data NDVI and SR and in situ measurements of leaf area index in mangrove forests (Kovacs et al., 2005; Kovacs et al., 2009). I chose also to use MSAVI2 (Modified Soil Adjusted Vegetation Index) as this index is known to correct for the signal caused by bare soil in sparsely vegetated areas, this index is expected to perform better for the dwarf and sparse sites (Qi et al., 1994). A map of the current LAI of the impoundment with RIM and the surrounding area can reveal information about the current state of the vegetation and can inform us whether the implementation of RIM resulted in a successful rehabilitation of the vegetation in the impoundment (i.e. no saltpans, less dwarf vegetation). These results cannot be compared over time, but the impounded area can be compared with the surrounding unmanaged mangroves. Secondly the impoundment with RIM can be compared with the impoundment that was already better reconnected to the Indian River Lagoon by the breaching of the dike (Verhoeven et al., 2014). For this purpose I correlated in situ LAI against several vegetation indices that can be found in Table 6. I excluded some field LAI measurements (15 out of 161) from the analysis as those were flooded areas in the June-2014 WV2 image.

Table 6. Vegetation indices tested against in situ LAI

Vegetation index	Formula	Band numbers
NDVI1	$\frac{NIR1 - RED}{NIR1 + RED}$	NIR1= 7 RED = 5
NDVI2	$\frac{NIR2 - RED}{NIR2 + RED}$	NIR2= 8 RED = 5
SR1	$NIR1/RED$	NIR1= 7 RED = 5
SR2	$NIR2/RED$	NIR2= 8 RED = 5
MSAVI 2	$\frac{2NIR1 + 1 - \sqrt{(2NIR1 + 1)^2 - 8(NIR1 - RED)}}{2}$	NIR1=7 RED=5

2.4.3. Statistical analysis

To assess classification accuracy, I calculated an error matrix, the percent accuracy and kappa statistics as well as user's and producer's accuracy (Congalton, 1991) . Producer´s accuracy is the error of omission (classifying as negative when positive – false negatives). The user´s accuracy is the error of commission (classifying as positive when negative – false positives). Kappa statistics refer to overall correct and incorrect classification rates and class-specific classification rates. The interpretation of Kappa statistics were done as follows <0.20 is poor, 0.21 < kappa < 0.40 fair, < kappa < 0.60 moderate, 0.61 < kappa < 0.80 good, and 0.81 < kappa < 1 very good (Landis and Koch, 1977).

I tested differences amongst percent cover for the different classes for the years 2008-2010, 2008-2014 and 2010-2014 for normality. I tested the pair-wise differences that met the assumption of a normal distribution using paired t-tests to assess whether there were significant differences in mean change in percent cover. The paired t-test tests the null hypothesis that the mean difference in values is 0 (Whitlock and Schluter, 2009). If this is not true, there is an indication that RIM had an influence on the vegetation.

In addition I tested the mean rate of change between the impoundment with RIM and the area outside the impoundment using student t-tests to see if there was a difference in the mean rate of change. The student t-test tests the null hypothesis that the difference in mean values is 0 (Whitlock and Schluter, 2009). Again, if this is not true, there is an indication that RIM had an influence on the vegetation.

I first tested the data for the assumptions of normality and equal variances. The rates of change I compared using Mann-Whitney tests in case of a non-normal distribution and/or non-equal variances. Unfortunately I could make no comparison between the reference impoundment (No RIM) as this impoundment was not captured on the 2008 image.

To establish a model of LAI, I used linear regression of several vegetation indices (NDVI1, NDVI2, SR1, SR2, MSAVI2) against the in situ LAI data to detect which one would best correlate field and impoundment scale LAI. F-tests for the slope were performed. I selected the model with the highest R^2 (i.e. highest explanatory power) and used it to produce a map of LAI. To see how the indices relate to each other I analyzed the correlation between indices by linear regression. All tests performed were significant at a level of $p<0.05$. I used STATISTICA 10 to calculate all the tests that were described above.

Results

3.1 Distribution and extent of mangrove vegetation

3.1.1. Vegetation spectra

Figure 5 shows vegetation spectra of the field classes after radiometric correction. The different categories of vegetation identified in the field (dwarf, sparse and dense types of black mangrove and herbaceous vegetation) show spectral signatures that suggest that they can be distinguishable in all three the types of remote sensing imagery. The DM image from 2008 has overall lower reflectance values than the UCX image from 2010, suggesting that radiometric correction did not deliver optimal results.

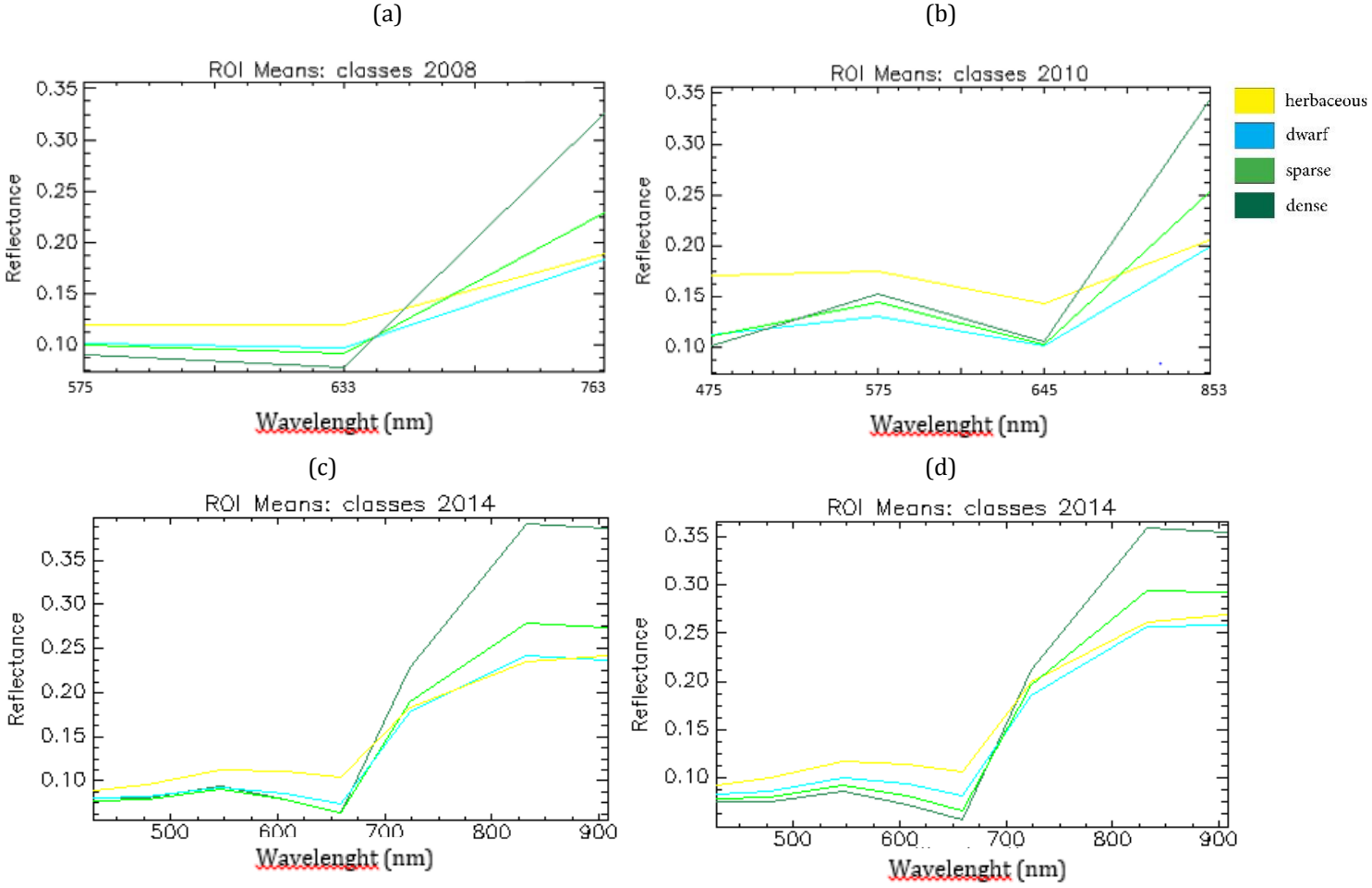

Figure 5. Spectral profiles for field classes: (a) DCM reflectance of the classes (b) UCX reflectance of the classes (c) pan-sharpened WV-2 (d) WV-2 reflectance. All spectra are means of the ROI's that were used as ground truth samples.

3.1.2. Land-cover classification: categories of NDVI

The NDVI values found for 2008 and 2010 are similar. The means, standard deviations and the established categories of NDVI values for all the classes of 2008 and 2010 can be found in Table 7.

Table 7. Mean and standard deviations of NDVI values for the different classes in the imagery of 2010, 2008, as well as the established categories of NDVI values.

2010	mean	stdv	Categories of NDVI values
herbaceous	0.16	+/-0.06	0.11 – 0.24
dwarf	0.33	+/-0.05	0.24 – 0.40
sparse	0.42	+/-0.05	0.40 – 0.47
dense	0.57	+/-0.07	0.47 – 1
2008			
herbaceous	0.16	+/-0.05	0.11 – 0.24
dwarf	0.33	+/-0.10	0.24 – 0.40
sparse	0.42	+/-0.03	0.40 – 0.47
dense	0.54	+/-0.05	0.47 – 1

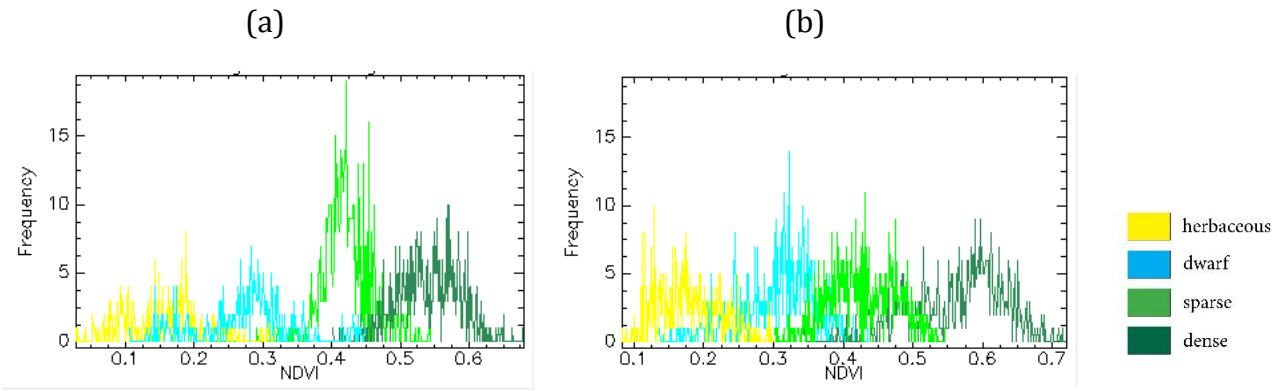

Figure 6. Histograms of NDVI values the different field classes: (a) 2008; (b) 2010

The classes that were distinguished in the field each have a unique distribution of NDVI values (Figure 6), a large part of the distributions approximate a normal distribution. Overlap between classes occurs mainly in the tails. Especially the herbaceous class in 2010 shows a skewed distribution, probably because the signal of this class will be most mixed with the spectral signal of soil. The dense class in 2010 is slightly bimodal, causing greater overlap with the sparse class.

3.1.3. Land-cover classification results 2008-2010

Table 8 shows the accuracies of the classifications made with the three categories representing density of mangrove vegetation and classes representing soil and herbaceous vegetation. Table 8 shows the users and producers accuracies of all the classes. User and producer accuracies of the dense class and the soil class are the highest for all the classifications. The dwarf mangrove class and the herbaceous class have low user's and producer's accuracies for both of the classifications. The majority of 2008 herbaceous class is misclassified as dwarf mangrove vegetation (298/514 pixels). For 2010 the sparse mangrove class has the lowest producer accuracy (313/1084 pixels are misclassified as dwarf). Overall accuracy of the classification of 2010 was higher than of the classification of 2008.

Table 8. Overall accuracy and kappa coefficient for the land-cover classifications as well as user's and producer's accuracy for the different density classes of the land-cover classifications for 2008 and 2010.

Year	Image	Classification accuracy	Kappa coefficient	Accuracy (%)	soil	herb.	dwarf	sparse	dense
2008	DM	79%	0.73	Producer's	96	35	88	61	99
				User's	94	66	61	95	84
2010	UCX	82%	0.78	Producer's	92	86	87	59	90
				User's	96	88	69	76	87

In Figure 7 the proportional cover for the classes of each land-cover classification is displayed. In Figure 7c the proportional cover for the non-impounded area shows that for both years the area outside the impoundments contains a much larger proportion of denser vegetation classes. The proportional cover for the impoundment with RIM are shown (Figure 7a) and compared to the proportional cover for the impoundment without RIM (Figure 7b). An increase in the dense mangrove class is found for the impoundment with RIM. In the unmanaged area outside the impoundments a more or less stable situation is found for both years with a very high proportional cover of the dense mangrove class. Between the years 2008 and 2010 the dense mangrove class in the impoundment with RIM increased by 37%. In 2010 the proportional cover of dense mangrove class was still much lower in the impoundment with RIM than it was in the impoundment without. The proportional cover of dense mangrove in 2010 was still much larger in the mangrove areas that are not impounded. In Figure 8 the resulting maps of the land-cover classification for the two years are shown.

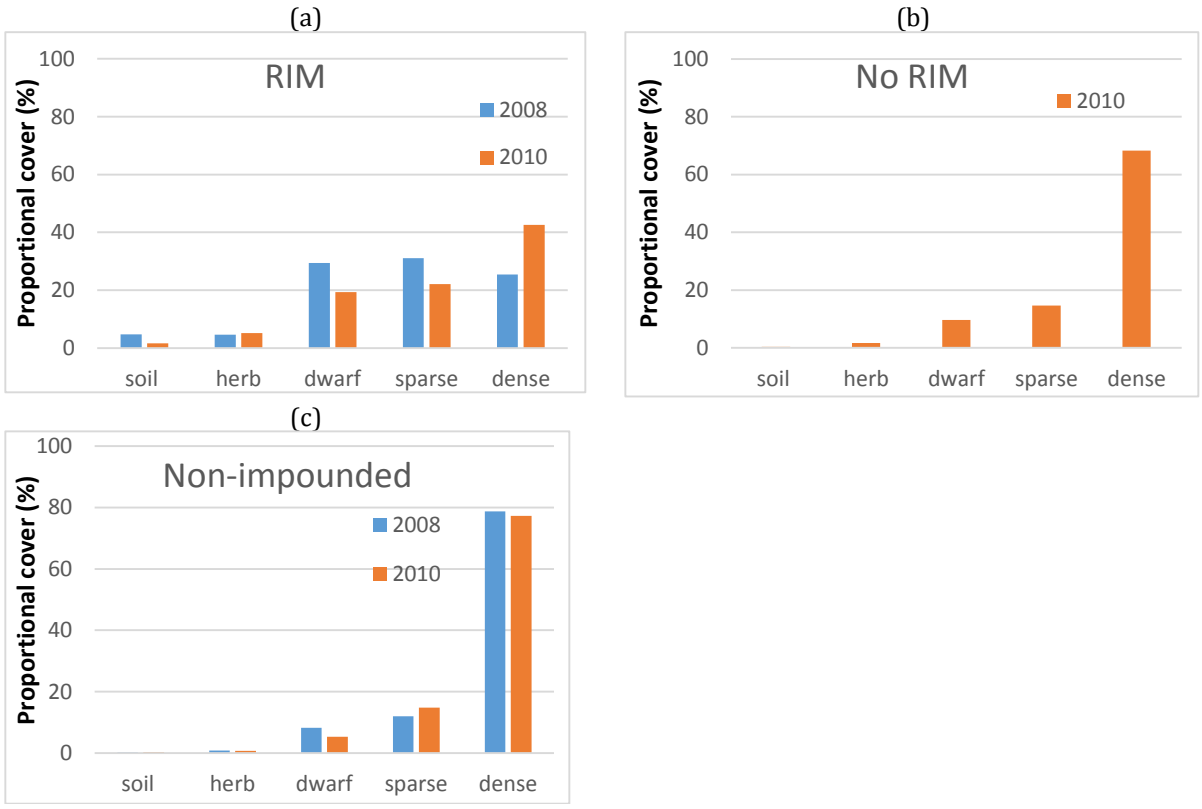

Figure 7. Proportional cover (%) of soil and vegetation density classes for the three areas that were studied: (a) impoundment with RIM; (b) the reference impoundment (No RIM) and (c) the non-impounded area.

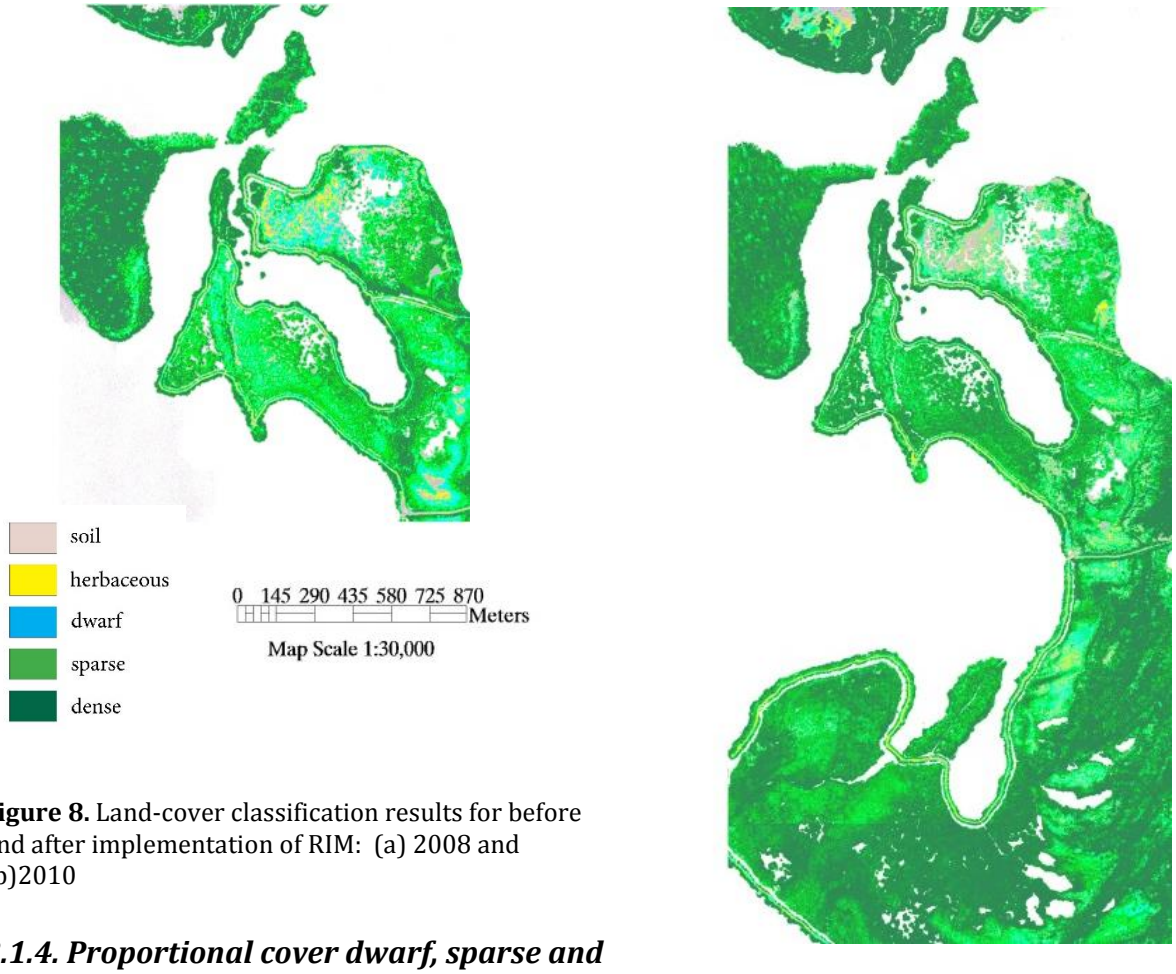

Figure 8. Land-cover classification results for before and after implementation of RIM: (a) 2008 and (b)2010

3.1.4. Proportional cover dwarf, sparse and dense sites

The proportional cover of the vegetation density classes for the dwarf, sparse and dense sites inside the impoundment with RIM for the years 2008, 2010 are presented in Figure 9. Especially, the dwarf sites inside the impoundment with RIM show a trend towards denser vegetation (Figure 9a). Moreover, the pattern of succession towards denser vegetation classes is visible (Figure10). Site 5, for example, (Figure 10g, h) contains little bare soil after implementation of RIM. For the sparse (Figure 9c) and dense sites (Figure 9e) a shift towards denser vegetation classes is evident.

Results from all statistical tests that were performed can be found in Appendix 4. There were no dwarf sites found in the non-impounded mangrove areas, for the sparse and dense sites control sites were found. No significant difference was found in mean rate of change (2008-2010) between the impoundment with RIM and the non-impounded area (Appendix 4). Paired t-tests showed significant differences within the dwarf sites before and after implementation of RIM (2008-2010): An increase in the dwarf mangrove class was shown to be significant (N=5, p=0.023). Also the decrease in the soil class was significant (N=5; p=0.013). No significant differences were found for the sparse and dense sites before and after RIM (Appendix 4).

A t-test showed that after implementation of RIM, a significantly larger proportion of dwarf mangrove vegetation was found in the reference impoundment than in the impoundment with RIM (N=5, p= 0.0017). No other significant differences were found between the dwarf sites in the two impoundments. There is, however, still a much larger proportional cover of bare soil on the dwarf sites in the impoundment with RIM than in the reference impoundment (31% vs. 2%). Possibly the difference was not significant due to the low number of sites (N=5) and the large variability. A t-test showed that on

the sparse sites a significantly larger extent of dwarf mangrove vegetation was found (N=5, p=0.047). The sparse sites in the reference impoundment show overall a more homogeneous cover of lower density mangrove (Figure 9d) than the sparse sites in the impoundment with RIM (Figure 9c).
It can be seen from the visual results of the classification (Figure 10) that the recovery of vegetation takes place on patches that were classified as bare soil in 2008. A decrease of 57 % of bare soil took place on the dwarf sites as well as an increase of 720% in the dwarf mangrove vegetation. The classification results also show an average increase of 79% in the dense mangrove vegetation that took place at the sparse sites and an increase of 24% in dense mangrove vegetation at the dense sites. However, these changes were not found to be significant, possibly again caused by a low number of sites (N=5) and large variability. In the non-impounded area a similar increase in dense mangrove took place at the sparse sites (63%) as took place at the sparse zones inside the impoundment with RIM. However, a decrease (12%) in dense mangrove took place at the dense sites.

(a)

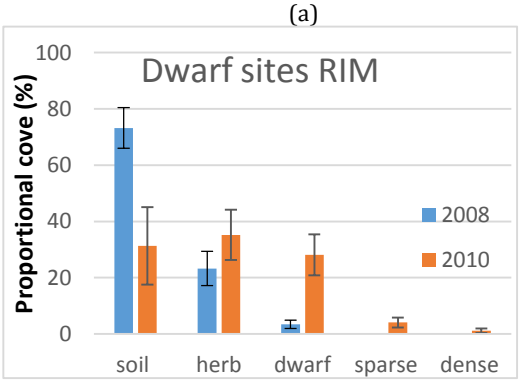

(b)

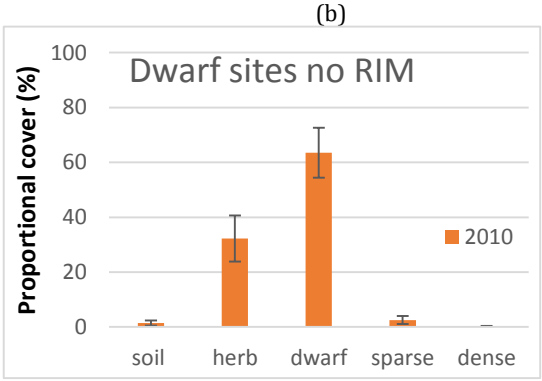

(c)

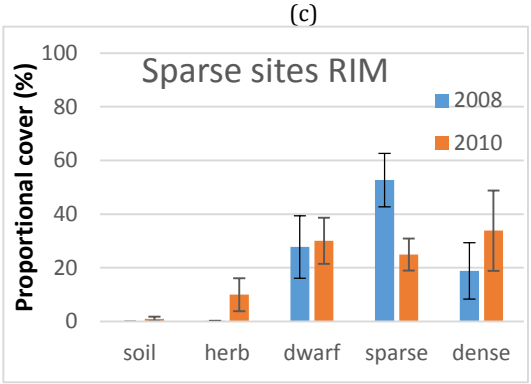

(d)

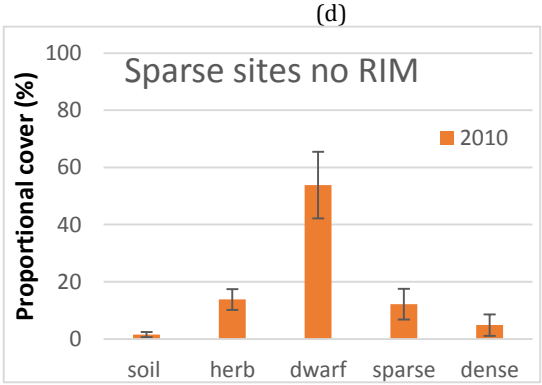

(e)

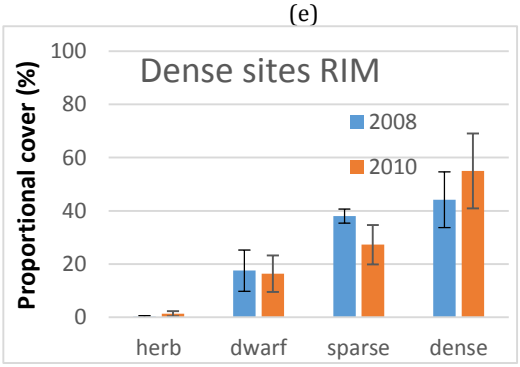

(f)

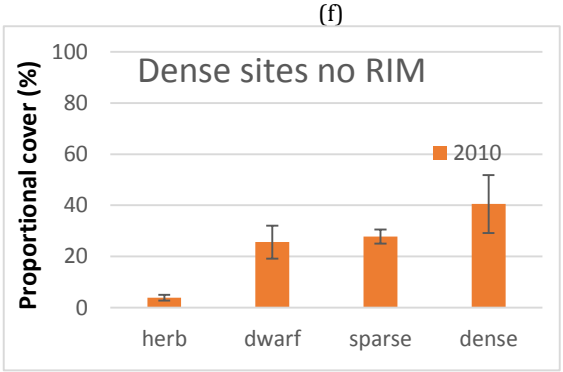

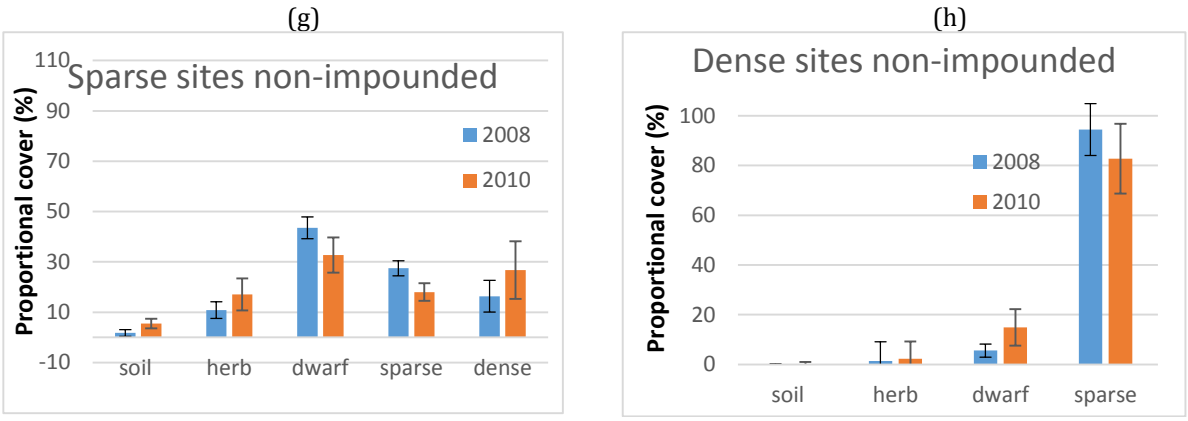

Figure 9. Proportional cover (%) of soil and vegetation classes for all zones, in the impoundment with RIM, the reference impoundment (no RIM) and the non-impounded area: (a) dwarf (RIM); (b) dwarf (no RIM); (c) sparse (RIM) (d) sparse (no RIM); (e) dense (RIM); (f) dense (no RIM); (g) Sparse (non-impounded); (h) Dense (non-impounded). Error bars indicate SE.

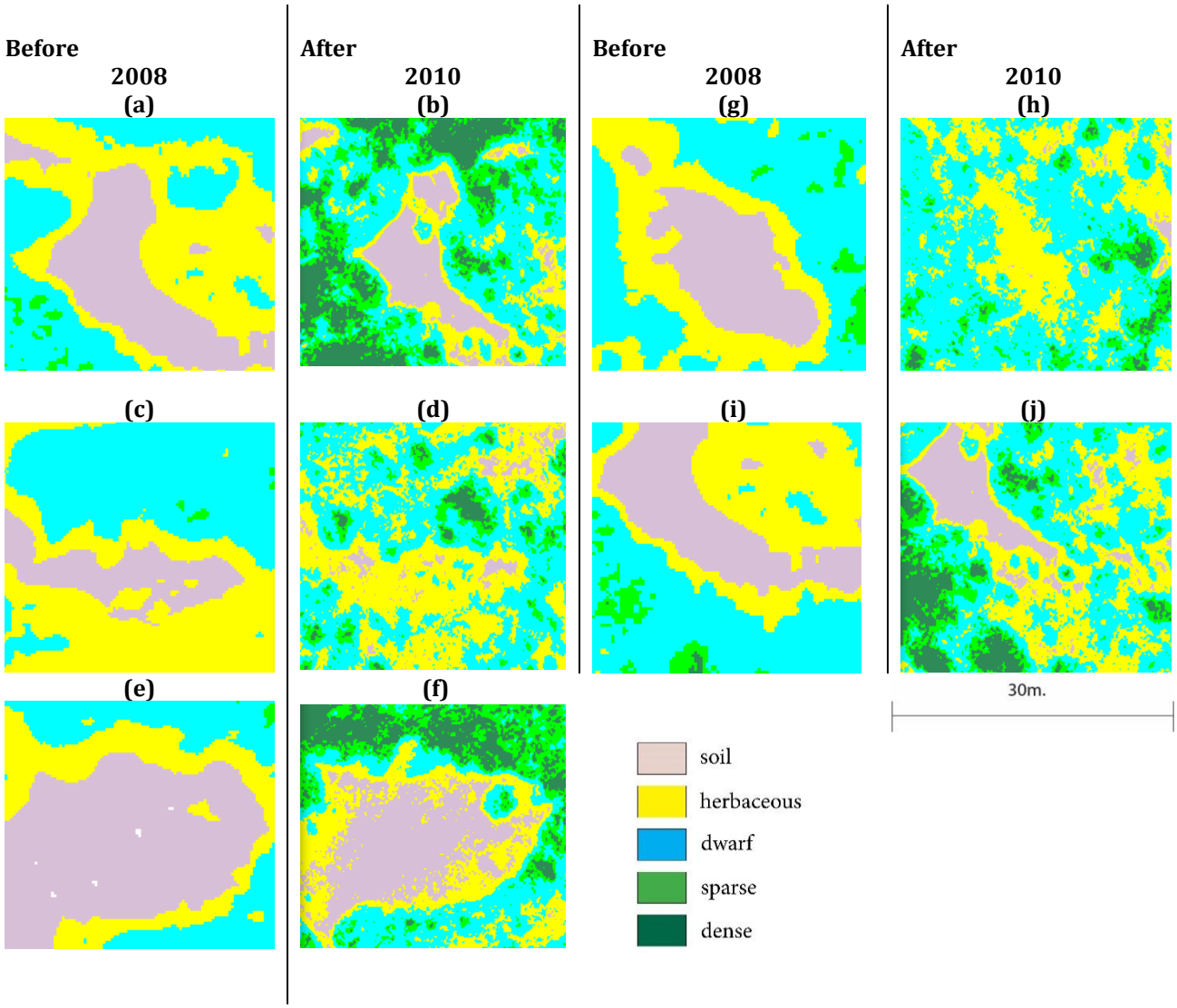

Figure 10. Classification results for all the dwarf sites inside the impoundment with RIM (2008 and 2010) (site 1 (a, b), site 3, (c, d), site 4 (e, f), site 5 (g, h) and site 6 (i, j))

3.1.5. Change detection

The most important change categories and the area of change are displayed in Table 9. From 2008 to 2010 an area of 5915 m^2 shifted from soil to vegetation. An area of 11692m^2 shifted from the herbaceous class to one of the mangrove classes. An area of 92756 m^2 shifted from a lower to a denser mangrove class.

Table 9. Change detection results, area of change between 2008 and 2010

	2008-2010 (m^2)
Soil-Vegetation	5915
Herbaceous-Mangrove	11692
Dwarf-sparse/dense	41031
Sparse-dense	51725

3.1.6. Land-cover classification 2014

NDVI values obtained from the WV2 image differed strongly from those of the airborne images, as much higher NDVI values were found for the same classes (Table 10). Established classes based on NDVI values can be found in Table 10 as well.

Table 10. Mean and standard deviations, and mean minus standard deviations of NDVI values for the different classes for the WV2 NDVI1

	Mean NDVI	**Stdv**	**Categories of NDVI values**
herbaceous	0.38	+/- 0.05	0.34 – 0.46
dwarf	0.53	+/- 0.04	0.46 – 0.59
sparse	0.62	+/- 0.03	0.59 – 0.67
dense	0.72	+/- 0.04	0.67 – 1

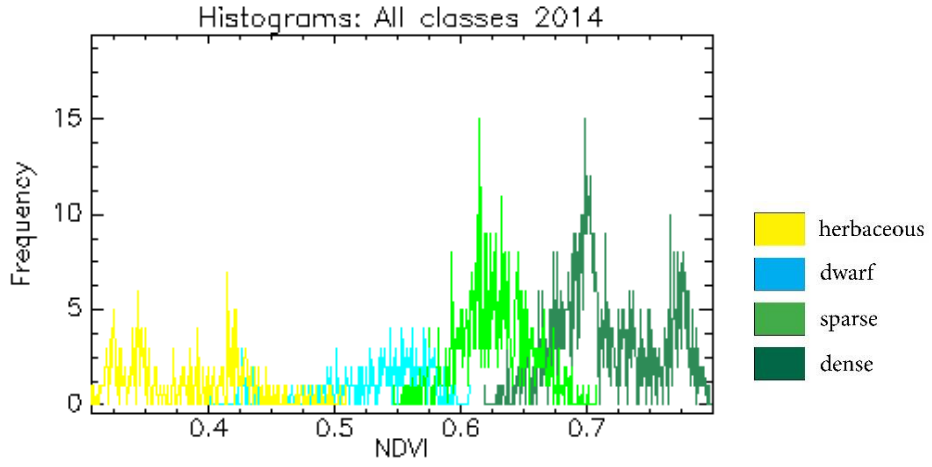

Figure 11: Histograms of NDVI values the different field classes of 2014

The NDVI values of 2014 also have distinct distributions (Figure 11) overlap between classes occurs mainly in the tails. Both the distributions of the herbaceous class and the dense mangrove class are bimodal.

3.1.7. Land cover classification results 2014

Classification accuracy is higher than the classification accuracies that were obtained for the aerial photographs (Table 11). Again, in 2014 the low density classes (herbaceous

and dwarf mangrove) have lower producer's and user's accuracies than the classes for soil and the denser mangrove classes.

Table 11. Overall accuracy and kappa coefficient for the land-cover classifications as well as user's and producer's accuracy for the different density classes of the land-cover classifications for 2014

Image	Classification accuracy	Kappa coefficient	Accuracy (%)	soil	herbaceous	dwarf	sparse	dense
WV2 0.5	82%	0.77	Producer's	83	75	74	79	97
			User's	98	85	60	85	92
WV2 2	83%	0.76	Producer's	85	79	73	64	99
			User's	100	69	59	90	88

Figure 12 displays the proportional cover of the vegetation classes found in the impoundment with RIM, the impoundment whitout RIM and the non-impounded area in 2014. The largest proportional cover of the classification inside the impounded areas are made up by sparse mangrove and dense mangrove, while the area outside is mainly covered by dense mangrove. In all areas a very low proportional cover is found for dwarf, herbaceous vegetation and soil. Figure 13 displays the map obtained for the land-cover classification of 2014.

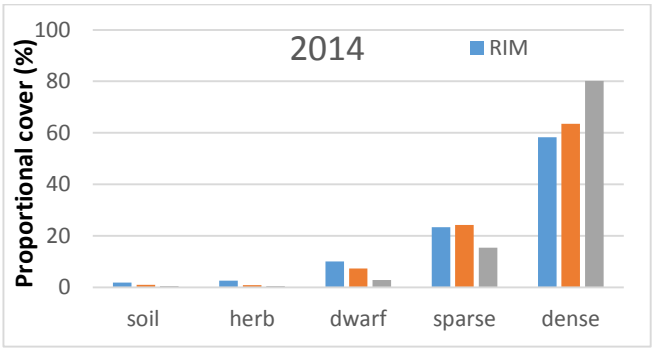

Figure 12. Proportional cover for each of the classes in the land-cover classification of 2014

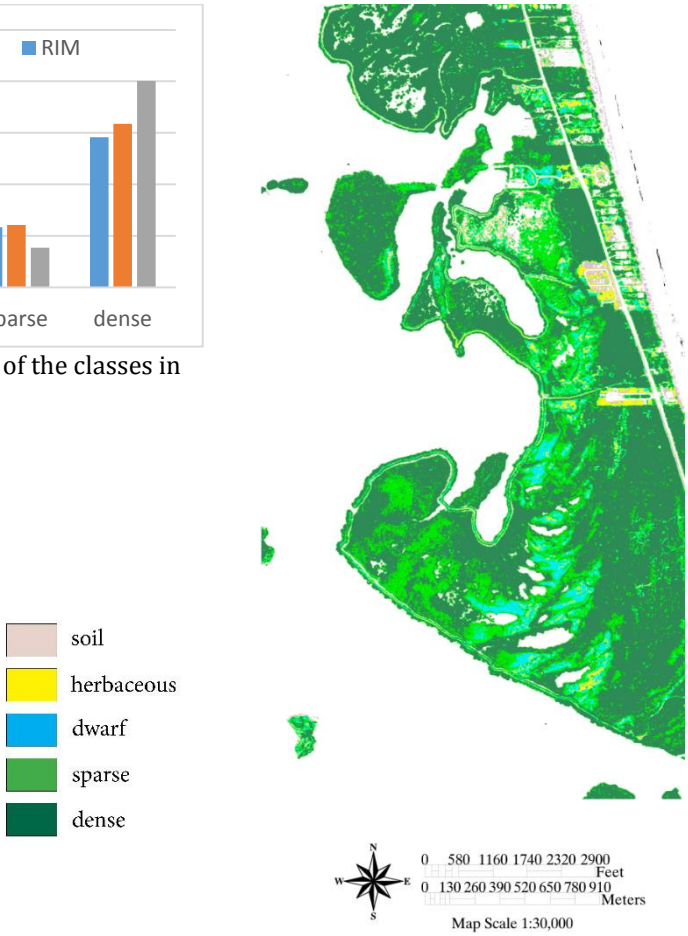

Figure13. Map with the land-cover classification results for the pan-sharpened WV2 image

3.1.8. Proportional cover sparse and dense sites 2014

Figure 14 shows the proportional cover for the sparse and dense sites in the classification of 2014. The sparse sites contain an almost homogeneous cover of sparse mangrove in the impoundment with RIM. The reference impoundment (No RIM) shows a larger proportion of dwarf mangrove. The dense sites inside both impoundments are rather similar with a large proportional cover of sparse mangrove and dense mangrove. Vegetation in the dense sites of the not impounded area is denser with a larger proportional cover of dense mangrove. In the reference impoundment (No RIM) the cover of the dwarf and sparse sites is very similar in 2010, while for 2014 this could not be assessed due to the standing water at the dwarf sites. In the classifications of 2010 and 2014 the impoundment with RIM contains a larger proportion with dense mangrove than the sparse sites in the reference impoundment.

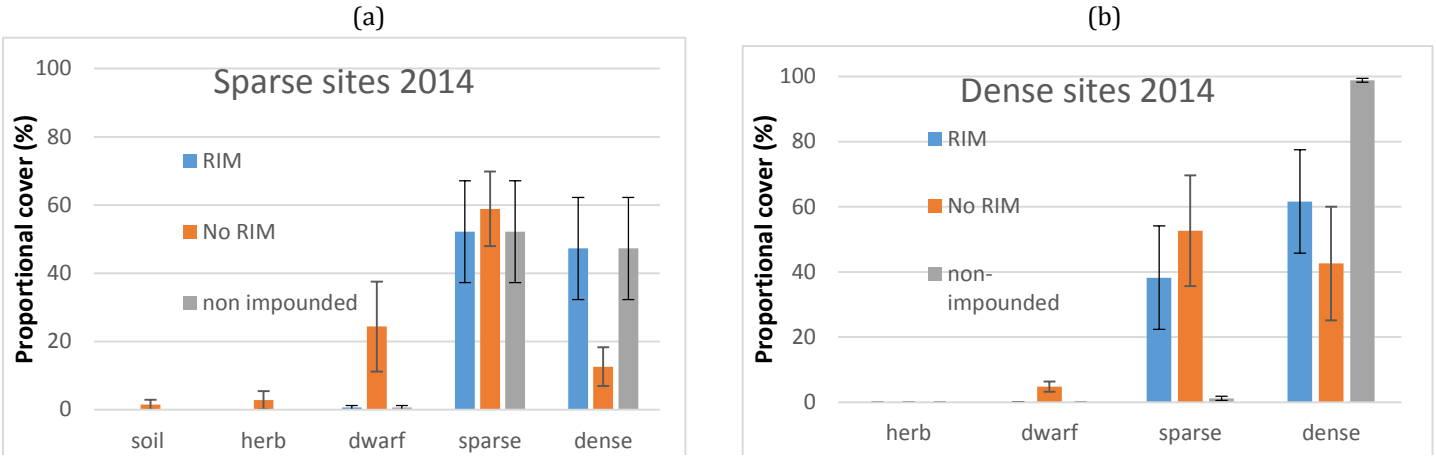

Figure 14. Proportional cover for the sparse (a) and dense (b) sites for the impoundment with RIM, no RIM and the non-impounded area in 2014. Error bars indicate SE.

3.1.9. Maximum likelihood classification 2014

The maximum likelihood classification had a lower accuracy than the density classification (78% accuracy and kappa Coefficient = 0.71). Producer and user accuracies of the maximum likelihood classification can be found in Table 12. The error matrix can be found in Appendix 3.

Table 12. User's and producer's accuracy for the different density classes of the Maximum likelihood classification for 2014

Image	Accuracy (%)	soil	herbaceous	dwarf	sparse	dense
WV2 0.5	Producer's	59	65	77	71	99
	User's	80	84	59	88	86

The proportional cover of the different mangrove areas in the maximum likelihood classification (Figure 15) resemble the land cover classification results obtained by the density slicing of NDVI values. An even higher proportional cover of the dense mangrove class is found in the non-impounded area. Also, a slightly higher proportional cover of bare soil is found for the impoundment with RIM.

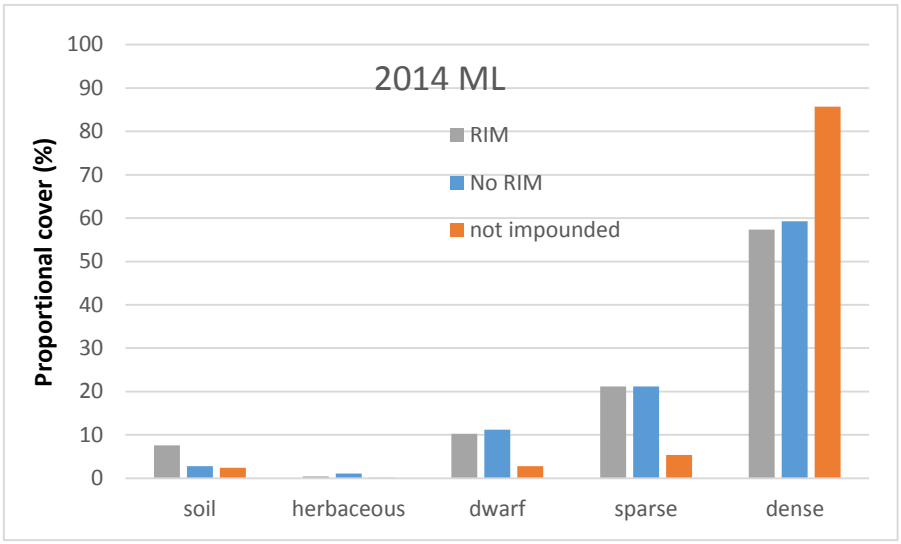

Figure 15. Proportional cover for each of the classes of the maximum likelihood classification of 2014

3.2. Productivity

3.2.1 Changes in Productivity 2008-2010

Before RIM (2008), mean NDVI was significantly lower than after RIM suggesting that with RIM productivity increased inside the impoundment. The result is in the opposite direction of the change measured in the non-impounded areas, where a significant, but slight decrease in NDVI is observed over the years 2008-2010 in the area outside the impoundments ($p<0.001$; Figure 16 and Table 13). Density classes showed similar significant increases in NDVI inside the impoundment with RIM in comparison with density classes outside, also suggesting increased productivity since the implementation of RIM.

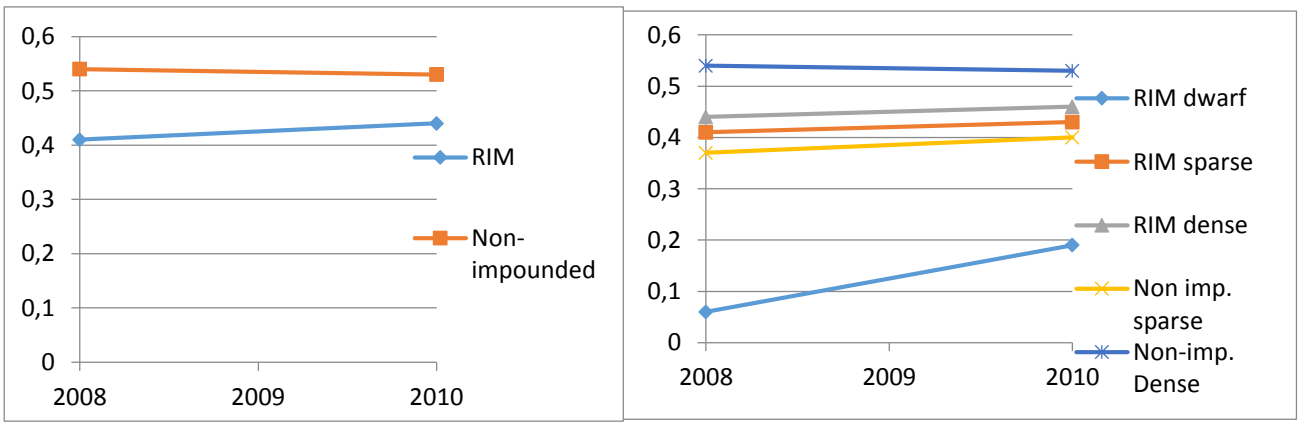

Figure 16. Mean NDVI values for RIM, non-impounded and all the sites inside the impoundment with RIM, as well as the sparse and dense sites in the non-impounded mangrove area.

Mean NDVI increased 8% from 2008-2010 inside the impoundment with RIM, while NDVI decreased 2 % in the unmanaged mangrove area outside the impoundments. For all the sites, dwarf, sparse and dense inside the impoundment with RIM the increase in NDVI is significant ($p<0.001$). For the dwarf sites the increase in NDVI is the largest: NDVI increased by 216%, versus 5 % and for both the sparse and dense sites. For the

dense control outside the impoundment with RIM, the NDVI decreased significantly, however, the sparse control sites show a similar increase in production as the sparse sites inside the impoundment with RIM (5%). No dwarf control site was found outside the impoundments. In both years NDVI is approximately 0.1 unit larger outside the impounded area.

Table 13. Mean NDVI for 2008 and 2010 for the whole impoundment, the unmanaged area outside the impoundment and the p-value of the dependent t-tests performed.

	Mean NDVI 2008	Mean NDVI 2010	p-value t-test
RIM	0.41	0.44	<0.001
Non impounded	0.54	0.53	<0.001
Dwarf	0.06	0.19	<0.001
Sparse	0.41	0.43	<0.001
Dense	0.44	0.46	<0.001
Sparse control	0.37	0.40	<0.001
Dense control	0.54	0.53	0.0013

3.2.2. Current state

Dense sites had higher in situ LAI values, followed by sparse and dwarf sites. The mean LAI recorded was 2.6, the average LAI value recorded for dwarf sites was 1.33, the average LAI value recorded for sparse sites was 2.54 and the average LAI value recorded for dense sites was 3.64.

Regression analyses of the in situ LAI (N=146) with several vegetation indices, including both normalized vegetation indices (NDVI1, NDVI2) and the simple ratios (SR1, SR2) revealed positive relationships (Figure 17; Table 14). All regression models developed fit the data quite well, and R^2 values suggest strong explanatory power. MSAVI2 is the least sensitive for changes in LAI at the higher values of LAI, followed by the both NDVI's that were tested. The F-tests for both models and t-test for the slope indicate that the linear models and b coefficients are all statistically significant. Both simple ratio's showed less saturation effects for high density of vegetation. The simple ratio (SR2) showed the strongest fit (R^2=0.71; F=359) and was therefore used to construct a map of leaf area index of the current state of both the impoundment with RIM and the impoundment without RIM.

Table 14. R^2, F-ratio, p-value, and SE-of estimate for the different linear models of the vegetation indices and in-situ LAI. Indices are listed from highest to lowest R^2 value.

	R^2	F-ratio	p-value	SE of estimate
SR2	0.71	359	<0.001	0.67
SR1	0.71	344	<0.001	0.68
NDVI 1	0.66	277	<0.001	0.73
NDVI 2	0.64	261	<0.001	0.75
MSAVI2	0.62	238	<0.001	0.54

(a)

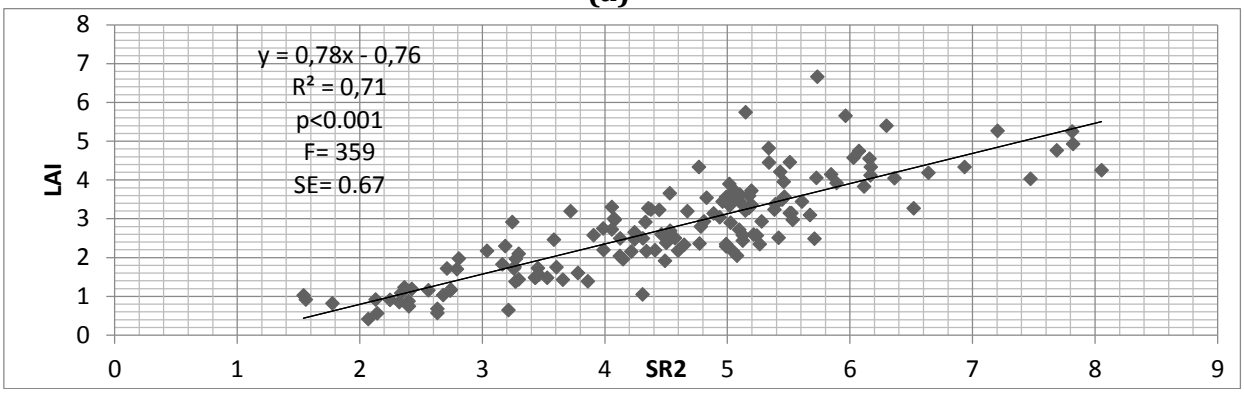
y = 0,78x - 0,76
R² = 0,71
p<0.001
F= 359
SE= 0.67
LAI
SR2

(b)

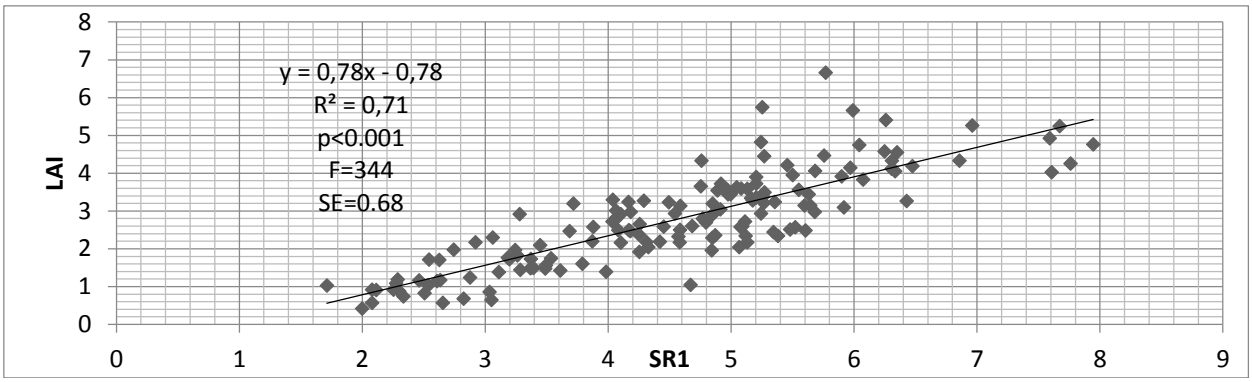
y = 0,78x - 0,78
R² = 0,71
p<0.001
F=344
SE=0.68
LAI
SR1

(c)

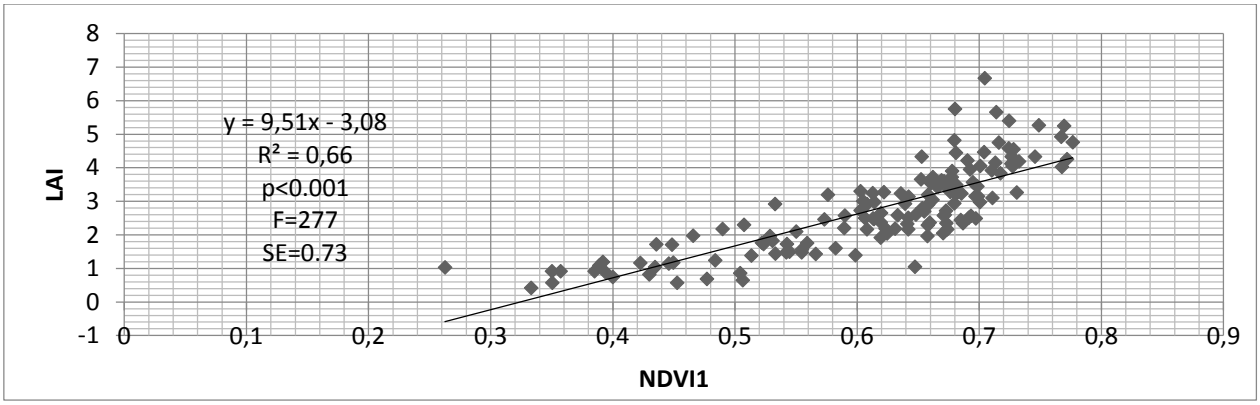
y = 9,51x - 3,08
R² = 0,66
p<0.001
F=277
SE=0.73
LAI
NDVI1

(d)

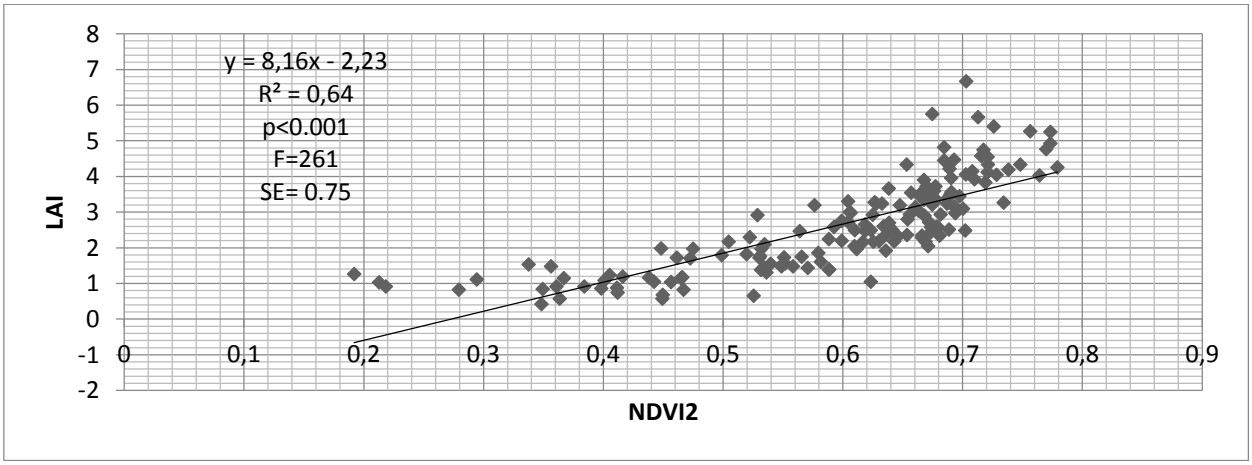
y = 8,16x - 2,23
R² = 0,64
p<0.001
F=261
SE= 0.75
LAI
NDVI2

(e)

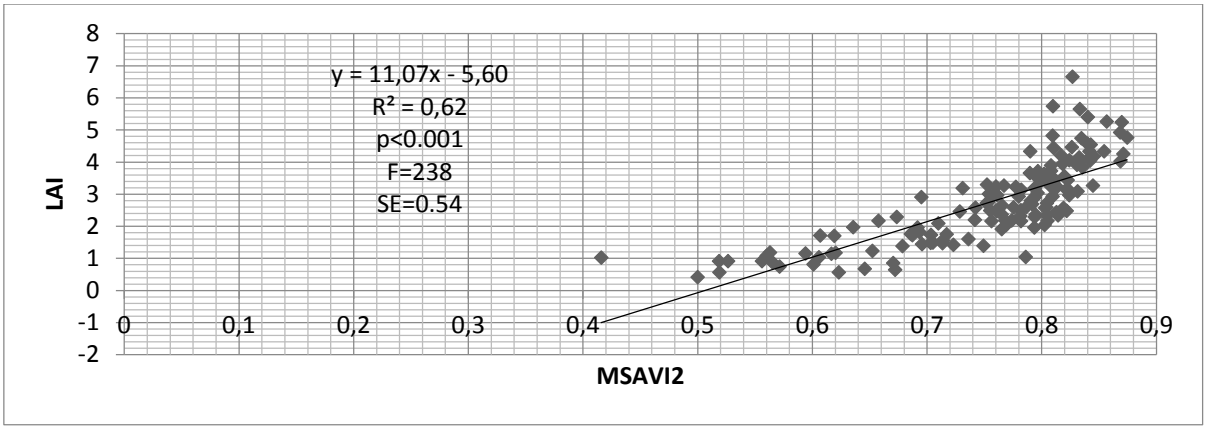

Figure 17. Prediction of leaf area index, using the simple ratio 2 (a), simple ratio 1 (b), NDVI1 (c), NDVI2 (d) and MSAVI2 (e) for the WV2 satellite image.

Based on the mapped estimates of LAI, an average LAI of 3.38 was found for the impoundment with RIM and an average LAI of 3.44 was found for the impoundment without RIM. These results suggest a sparse to dense cover of mangrove for both impoundments. The mean predicted LAI found in the unmanaged mangrove area outside both impoundments was 4.58, suggesting an overall denser cover of mangrove vegetation. These findings relate closely to the land cover classification that was established for 2014, in which both impoundments have a similar proportional cover of sparse mangrove and dense mangrove. This is perhaps because the vegetation index used for the land cover classification (NDVI1) and the vegetation index used for the LAI map are highly correlated (R^2=0.95; Table 15). The results from the land cover classification suggest a denser cover outside the impoundments as the area outside the impoundments contains a much larger proportion of dense mangrove.

Table 15. R^2 for the correlation between indices.

	SR2	**NDVI1**	**NDVI2**	**MSAVI2**
SR1	0.98	0.95	0.86	0.86
SR2		0.95	0.89	0.85
NDVI1			0.98	0.99
NDVI2				0.95

The zonation of mangrove vegetation can clearly be seen from the LAI map in Figure 18. It can also be seen that vegetation in the impoundments becomes sparser land-inward, where also larger areas with dwarf and herbaceous vegetation are found. The denser vegetation that can be seen eastward of the sparser mangrove area is the upland forest which has higher values of LAI than the sparser mangrove areas (pink line in figure 18c represents the border with the upland forest).

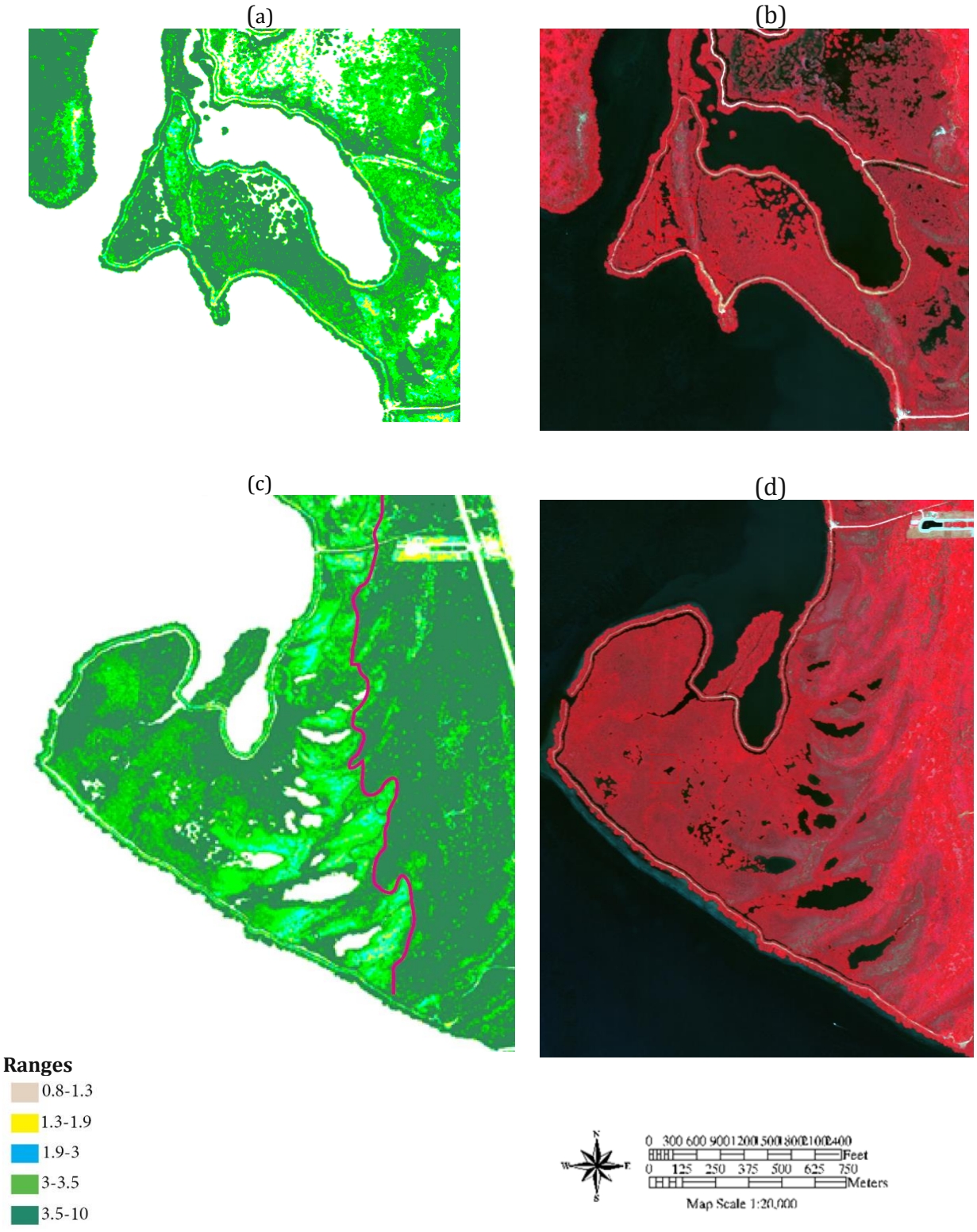

Figure 18. LAI map the impoundment with RIM (a) and 23 (c), a false color composite image (NIR1, Red, Green) of the impoundment with RIM (b) and 23 (d) from the WV2 image next to it.

4. Discussion

4.1. Distribution and extent of mangrove vegetation

In the present study the effects of rotational impoundment management on a mangrove ecosystem were investigated with the use of remote sensing. Changes in the extent and distribution, productivity and state of the mangrove vegetation were followed and quantified over time to see if these were influenced by the implementation of RIM.
On the dwarf sites, the sites inside the impoundments characterized by hypersaline conditions and by low black mangrove vegetation or without cover, the greatest changes in distribution and extent of mangrove and herbaceous vegetation took place. On average, 57% of bare soil on dwarf sites were re-colonized by herbaceous and dwarf and intermediate mangrove vegetation. The lowest density mangrove increased seven times from its initial pre-RIM proportional cover. This result shows the succession on the dwarf sites towards denser vegetation. I also observed succession towards denser vegetation at the sparse sites; however, these shifts were not statistically significant as a similar transition was found in sparse sites in the non-impounded area. The succession towards denser vegetation classes in the area with RIM partly confirm the visual observations in the field by Verhoeven et al. (2014). This is likely because plant community composition in mangrove areas is mainly controlled by salinity (Stringer et al. 2010), with highest ground water salinities in salt pan and dwarf mangrove areas, followed by the sparse black mangrove areas, dense black mangrove and the fringes with red mangrove. Black mangroves tolerate high salinity conditions by actively excreting salt from the leaves but, as suggested by Atkinson et al. (1967) this active process requires energy from the mangroves, thus also limiting growth of these species under very high salinity conditions. Salinity induced stress increases demand for nitrogen (Feller et al., 2003). Black mangroves are dominant in areas where salinity levels approximate those of sea water where growth of black mangroves is stunted and limited under hypersaline conditions (Verhoeven et al., 2014). Feller et al. (2003) found a greatest response of dwarf sites to the addition of extra nitrogen to impounded mangroves, probably because these sites had the highest salinity stress. The implementation of RIM caused salinity levels to lower and plant extractable nitrogen to increase (Verhoeven et al., 2014), both factors are probably related to the changes in land-cover I observed at dwarf and sparse sites. Why sparse sites in the non-impounded area also show an increase in the denser mangrove is not known, as no ground control data is available for those sites. A possible explanation could be recovery from a hurricane that took place in 2004 (Vogt et al., 2012).

Feller et al. (2003) found that photosynthetic activity, leaf production and shoot growth increased when the system was fertilized with additional nitrogen on all types of sites (dwarf, sparse and dense). However, more recent results showed no notable change in leaf production, despite increased plant available nitrogen in the soil and increased nitrogen content in the leaves (Verhoeven et al., 2014). My land-cover classification results do show an average increase of 24% in the denser mangrove but again this change was not significant. This increase in the denser mangrove class could thus be explained by either a change in nitrogen content of the leaves, or by the fact that, despite the findings of Verhoeven et al. (2014), productivity did increase.

Over the whole impounded area with RIM, the dense mangrove increased 67% between 2008 and 2010. This indicates a succession towards denser vegetation on the scale of the impoundment. As this shift is not observed in the non-impounded area, it is partly related to the implementation of RIM because of the changes this management regime induced in salinity and freshwater availability. In 2010 overall density of mangrove vegetation is still higher in the reference impoundment. Moreover, no dwarf sites were found in the non-impounded areas, suggesting that the hypersaline conditions are a characteristic of impounded mangrove areas (Feller et al., 2003). In 2014 the extent of mangrove vegetation in the impoundment with RIM and the reference impoundment is similar. The reference impoundment did not have distinct salt pan areas (Verhoeven et al., 2014) and this is probably why vegetation cover was overall higher than in the impoundment that had RIM implemented. Both maximum likelihood and density-based classifications for 2014 show a gradient from sparse to dense cover in both the impounded areas (RIM and no RIM). Overall classification accuracy was quite high for both classifications, making the results that are obtained reliable. However, at the time of the collection of the WV2 image (June 2014) the dwarf sites were flooded and the eutrophic standing water interfered with the results, making a part of the analysis, especially on those sites that showed the greatest change over 2008-2010, impossible for 2014.

All results clearly showed a higher fraction of the densest category of mangrove vegetation in the non-impounded areas. This suggests that even though there have been efforts to rehabilitate the impounded mangrove areas it has not been sufficient to completely restore the mangrove vegetation to an extent/distribution that would have been there without the impoundments. However, during the continuous flooding of the impoundments, species dominance shifted to red mangrove as this species is more tolerant to flooding (Rey et al., 2009). Part of the shift in density that is found over the whole impoundment might thus also be due to an increase in red mangrove or increasing stature of the red mangrove stands. Red mangrove has on average higher LAI values (Kovacs et al., 2005), and this might also be associated with a greater fraction of the densest mangrove class at the non-impounded area. Red mangrove leaves are dark green, have a thick and leathery structure and are 6 to 12 cm long. Black mangrove leaves are slightly smaller, 3 to 12 cm (Hogarth, 2015) probably causing on average lower LAI values for this species (Kovacs et al., 2005). Unfortunately, no ground truth data was available on the different mangrove species to allow species level classifications. The human eye has limited capability to distinguish mangrove species by visual interpretation of high resolution imagery (Keunzer et al., 2011) and this would likely increase uncertainty in the classification. Anecdotal observations during our field campaign showed, however, red mangrove under the canopy of dense black mangrove, making a shift in species dominance an unlikely explanation for the increase in the denser classes in the land-cover classification.

4.2. Changes in productivity (2008-2010)

I found opposing patterns of change in NDVI in RIM and non-RIM areas. NDVI significantly increased in all study sites as well as over the whole impoundment with RIM, and it significantly decreased in the non-impounded area. These results suggest that the increase in productivity in the impoundment with RIM is probably due to the implementation of RIM. I discarded the effects of fluctuations in seasonal variability or changes caused by distortion in the remote sensing imagery in our results because control regions showed less changes as well as changes in the opposite direction. The

slight decrease in NDVI observed in the non-impounded area was possibly caused by climatic variability. On average 2010 was colder and dryer year than was 2008 (Appendix 1). Lower temperature and especially lower precipitation levels can have a negative influence on the productivity of mangrove vegetation in the region where the study took place (Verhoeven et al., 2014). It could be that the less favorable climatic conditions have suppressed the productivity inside the impoundment with RIM as well. However, due to the artificial pumping of the estuarine water into the impoundment precipitation level in the wet season (late spring and summer; Appendix 1) is expected to have less influence on the water levels inside the impoundment than in a system that is mainly controlled by natural tidal inundation.
The biggest change in productivity was an increase in mean NDVI (216%) for the dwarf sites. This large shift in productivity is probably mainly due to the increase of herbaceous and low mangrove vegetation in areas with hypersaline conditions before RIM, as was found in the results of the land-cover classification. The time series of MODIS NDVI of both impoundments, constructed by Silvestri et al. (2014) did not show this change in mean NDVI from 2008-2010 probably due to the low spatial resolution (250m).

4.3. Current state: mangrove vegetation

Mapping leaf area index is an established method to scale local field results to the scale of a mangrove forest (Kovacs et al., 2009; Kovacs et al., 2005), and in this case a mangrove impoundment. Leaf-area index is related to productivity of the vegetation (Pu and Cheng, 2015), the field level measurement gives an indication of the density of the forest, and therefore of its condition. There are not many records of LAI in mangrove forests (Kovacs et al., 2009) and LAI strongly differs between species of mangrove and their condition and even for healthy stands mangrove LAI is quite low in comparison to terrestrial forests (Kovacs et al., 2009). Healthy stands of red mangrove can have mean LAI up to 5.7 (Araujo at al., 2009) but much lower mean values have also been reported (2.49; Kovacs et al., 2005). Black mangrove shows even lower LAI values, ranging from 2.7 to 3.2 (Ramsey and Jensen, 1996), or between 2.39 in dwarf stands and poor condition black mangrove to 4.66 in healthy black mangrove (Kovacs et al., 2009). In this study we found a mean LAI of 2.6 (ranging between 1.33 and 3.64), which approximates the values found for dwarf and sparse stands found by Kovacs et al. (2009).
The mapped estimates of leaf area index showed similar results as the land-cover classification, in which a gradient of sparse to dense cover exists in the impounded areas and a much denser cover is found in the non-impounded area. The mean LAI mapped for the area with RIM (3.38) approximates values found for sparse to dense black mangrove ecosystems (Kovacs et al., 2009). One possible explanation for the differences to the non-impounded area is that there is a greater extent of red mangrove, but additional field data is required to confirm this possibility. It must be noted that there were nine months between the collection date of the WV2 images and the collection of field data, in which changes could have taken place in the measured leaf area index. Despite this fact, strong correlations were found between the *in situ* LAI and the vegetation indices used suggesting that even if there were changes in LAI over these 9 months, they were likely negligible.

4.4. Recommendations for future studies

This study has scaled up the local field results to the impoundment and the methodology described could be employed to investigate changes in mangrove extent and productivity in several impoundments. This would inform on the changes in mangrove vegetation caused by RIM.

Additional spatial information such as image segmentation could improve classification results. Using image segmentation and characteristics of classes beyond solely spectral information is known to increase classification accuracy of mangrove forest (Heenkenda et al., 2014; B. W. Heumann, 2011). I tried image segmentation on the orthophotographs but the results were not satisfactory, and therefore I opted to leave this analysis out. In addition Pu and Cheng (2015) report a better correlation between LAI and spectral indices in combination with textural information from Worldview-2; future work should investigate whether a more accurate representation of LAI could be achieved using additional textural information in mangrove ecosystems.

5. Conclusion

The implementation of rotational impoundment management in a mangrove area in Florida has caused changes in the distribution and state of the vegetation. Large shifts were found in vegetation at areas isolated from the tide with hypersaline conditions. The supply of lagoon water in the summer is a normal feature for natural mangrove systems located in the Indian River Lagoon, as these areas are subject to tidal water exchange (Verhoeven et al., 2014). Summer water levels in the Indian River Lagoon are generally higher do to thermal expansion and an increase in precipitation levels. After the implementation of RIM an increase in herbaceous vegetation and lower mangrove vegetation was shown at the areas that were isolated from the tide. Moreover, a succession towards denser mangrove vegetation and/or an increase in productivity was also observed at areas that already had a sparse to dense cover of black mangrove vegetation.

A map of the leaf area index of the impoundment five years after the implementation of rotational impoundment management showed a sparse to dense cover of mangrove vegetation. Denser mangrove vegetation was located on the side of the lagoon, while land-inward mangrove vegetation became sparser. The mangrove area that was not impounded showed an overall denser cover of mangrove vegetation, possibly related to a different distribution of species (i.e. a higher fraction cover of red mangrove) or a denser cover of the dominant black mangrove. It was shown that RIM was beneficial overall for the growth of mangrove vegetation and caused a re-establishment of vegetation in areas that were hypersaline before.

Works cited

ASDinc, Analytical Spectral Devices inc., 2002. Fieldspec pro user guide. 1-136

Atkinson, M. R., Findlay, G. P., Hope, a B., Pitman, M. G., Saddler, H. D. W., West, K. R., 1967. Salt regulation in the mangroves, Australian Journal of Biological Sciences, 20, 589–599

Ball, M. C., 2002. Interactive effects of salinity and irradiance on growth: Implications for mangrove forest structure along salinity gradients. Trees - Structure and Function, 16(2-3), 126–139

Brockmeyer, R.E., Rey, J., Virnstein, R.W., Gilmore, R.G., Earnest, L., 1996. Rehabilitation of impounded estuarine wetlands by hydrologic reconnection to the Indian River Lagoon, Florida (USA). Wetlands Ecology and Management, 109, 93–109

Chen, H. M., Arora, M. K., Varshney, P. K., 2003. Mutual information-based image registration for remote sensing data. International Journal of Remote Sensing, 24(18), 3701–3706

Christopherson, J., 2010. USGS quality assurance plan for digital aerial imagery Certification Report for the Microsoft Vexcel UltraCamD , UltraCamX , UltraCamXp , and UltraCamXp WA Models

Conchedda, G., Durieux, L., Mayaux, P., 2008. An object-based method for mapping and change analysis in mangrove ecosystems. International Journal of Photogrammetry and Remote Sensing, 63(5), 578–589

Congalton, R. G., 1991. A review of assessing the accuracy of classifications of remotely sensed data. Remote Sensing of Environment, 37(1), 35–46.

Debez, A., Saadaoui, D., Slama, I., Huchzermeyer, B., Abdelly, C., 2010. Responses of Batis maritima plants challenged with up to two-fold seawater NaCl salinity. Journal of Plant Nutrition and Soil Science, 173(2), 291–299

Decagon Devices, 2013. AccuPAR PAR / LAI Ceptometer Model LP-80

Facchi, A., Baroni, G., Boschetti, M., Gandolfi, C., 2012. Comparing Opticaland Direct Methods for Leafarea Index Determination in a Maize Crop. Journal of Agricultural Engineering, 41, 33–40

Feller, I. C., Whigham, D. F., McKee, K. L., Lovelock, C. E., 2003. Nitrogen limitation of growth and nutrient dynamics in a disturbed mangrove forest, Indian River Lagoon, Florida. Oecologia, 134(3), 405–414. http://doi.org/10.1007/s00442-002-1117-z

Floore, T.G., 2006. Mosquito Larval Control Practices: Past and Present. Journal of the American Mosquito Control Association, 22(3), 527–533

Gamon, J. A., Field, C. B., Goulden, M. L., Griffin, K. L., Anne, E., Joel, G., 2015. Ecological Applications, 5(1), 28–41

Geneletti, D., Gorte, B. G. H., 2003. A method for object-oriented land cover classification combining Landsat TM data and aerial photographs. International Journal of Remote Sensing, 24(6): 1273–1286

Hansen, P. M., & Schjoerring, J. K., 2003. Reflectance measurement of canopy biomass and nitrogen status in wheat crops using normalized difference vegetation indices and partial least squares regression. Remote Sensing of Environment, 86(4), 542–553

Heenkenda, M., Joyce, K., Maier, S., & Bartolo, R., 2014. Mangrove Species Identification: Comparing WorldView-2 with Aerial Photographs. Remote Sensing, 6(7), 6064–6088

Heumann, B. W., 2011a. Satellite remote sensing of mangrove forests: Recent advances and future opportunities. Progress in Physical Geography, 35(1), 87–108

Heumann, B.W., 2011b. Remote sensing of mangrove composition and structure in the Galapagos Islands (Doctoral dissertation). Retrieved from the Carolina Digital Repository

Heumann, B. W. 2011a. An object-based classification of mangroves using a hybrid decision tree-support vector machine approach. Remote Sensing, 3(11), 2440–2460

Hirata, Y., Tabuchi, R., Patanaponpaiboon, P., Poungparn, S., Yoneda, R., Fujioka, Y., 2013. Estimation of aboveground biomass in mangrove forests using high-resolution satellite data. Journal of Forest Research, 19(1), 34–41

Hoghart, 2015, P.J. The biology of mangroves and seagrasses, 3, Oxford, UK, Oxford University Press

Honkavaara, E., Arbiol, R., Markelin, L., Martinez, L., Cramer, M., Bovet, S., Veje, N., 2009. Digital Airborne Photogrammetry—A new tool for quantitative remote sensing? A state-of-the-art review on radiometric aspects of digital photogrammetric images. Remote Sensing, 1(3), 577–605. 14

Huete, A., 2014. Vegetation indices,Encyclopedia of Remote Sensing, Encyclopedia of earth sciences series 2014, 883-886

Humphrey, J., 2011. An optional color infrared project: USGS program Florida minimum technical standards for mapping projects, Survey & Map Report. (2010625)

Intergraph, 2009. Digital mapping camera system

Jacobsen, K. 2003. Mapping with IKONOS images, Geoformation for European-wide Integration, Benes (ed.), Millpress, Rotterdam, 149–156

Johnson, B., 2014. Effects of Pansharpening on Vegetation Indices ISPRS, International Journal of Geo-Information, 3, 507-522

Johnston, R.M. and Barson M.M., 1993. Remote sensing of Australian wetlands: an evalutation of Landsat TM data for inventory and classification. Australian Journal of Marine and Freshwater Resources 44, 235-252

Kovacs, J. M., King, J. M. L., Flores de Santiago, F., Flores-Verdugo, F., 2009. Evaluating the condition of a mangrove forest of the Mexican Pacific based on an estimated leaf area index mapping approach. Environmental Monitoring and Assessment, 157, 137–149

Kovacs, J. M., Wang, J.,Flores-Verdugo, F., 2005. Mapping mangrove leaf area index at the species level using IKONOS and LAI-2000 sensors for the Agua Brava Lagoon, Mexican Pacific. Estuarine, Coastal and Shelf Science, 62(1-2), 377–384

Krause, G., Bock, M., Weiers, S., Braun, G. 2004. Mapping land-cover and mangrove structures with remote sensing techniques: a contribution to a synoptic GIS in support of coastal management in North Brazil. Environmental Management, 34(3), 429–440

Kuenzer, C., Bluemel, A., Gebhardt, S., Quoc, T. V., Dech, S., 2011. Remote Sensing of Mangrove Ecosystems: A Review. Remote Sensing 3, 878–928

Kumar, L., Schmidt, K., Dury, S., Skidmore, A., 2010. Imaging spectrometry and vegetation science, Imaging Spectrometry Basic Principles and Prospective Applications, Springer Netherlands, 111-156

Laanbroek, H.J., Keijzer, R.M., Verhoeven, J.T.A., Whigham, D.F., 2012. The Distribution of Ammonia-Oxidizing Betaproteobacteria in Stands of Black Mangroves (Avicennia germinans). Frontiers in Microbiology, 3, 1-11

Landis, J.; Koch, G., 1977. The measurement of observer agreement for categorical data. Biometrics 33, 159–174

Lehmann, J., Nieberding, F., Prinz, T., Knoth, C., 2015. Analysis of Unmanned Aerial System-Based CIR Images in Forestry—A New Perspective to Monitor Pest Infestation Levels. Forests, 6(3), 594–612

Lee, T. M., Yeh, H. C., 2009. Applying remote sensing techniques to monitor shifting wetland vegetation: A case study of Danshui River estuary mangrove communities, Taiwan. Ecological Engineering, 35(4), 487–496

Marchand, C., Baltzer, F., Lallier-Vergès, E., Albéric, P., 2004. Pore-water chemistry in mangrove sediments: relationship with species composition and developmental stages (French Guiana). Marine Geology, 208(2-4), 361–381

Manakos, I., Manevski, K., Kalaitzidis, C., Edler, D., 2011. Comparison Between FLAASH and ATCOR Atmospheric Correction Modules on the Basis of Worldview-2 Imagery and In Situ Spectroradiometric Measurements. EARSeL 7th SIG-Imaging Spectroscopy Workshop

Myneni, R.B., Williams, D.L, 1994. On the Relationship between FAPAR and NDVI. Remote sensing of Environment, 211, 200-211

Ozesmi, S. L., Bauer, M. E., 2002. Satellite remote sensing of wetlands. Wetlands Ecology and Management, 10(5), 381–402

Padwick, C., Deskevich, M., Pacifici, F., Smallwood, S., 2010. Worldview-2 pan-sharpening, ASPRS Annual conference, April 26-30-2010, San Diego

Pu, R., Cheng, J., 2015. Mapping forest leaf area index using reflectance and textural information derived from WorldView-2 imagery in a mixed natural forest area in Florida, US. International Journal of Applied Earth Observation and Geoinformation, 42, 11–23

Pu, R., Landry, S., 2012. A comparative analysis of high spatial resolution IKONOS and WorldView-2 imagery for mapping urban tree species. Remote Sensing of Environment, 124, 516–533

Qi, J., Chehbouni, a., Huete, a. R., Kerr, Y. H., Sorooshian, S., 1994. A modified soil adjusted vegetation index. Remote Sensing of Environment, 48(2), 119–126.

Rey, J., O'Connell, S.M., Carlson, D.B., Brockmeyer Jr., R.E., 2009. Characteristics of mangrove swamps managed for mosquito control in eastern Florida, USA: a re-examination. Marine Ecology Progress Series, 389(2), 295–300

Rey, J.R., Walton, W.E., Wolfe, R.J., Connelly, C. R., O'Connell, S.M., Berg, J., Sakolsky-Hoopes, G.E., Laderman, A.D. 2012. North American wetlands and mosquito control. International journal of environmental research and public health, 9(12), 4537–605

Rey, J.R., Crossman, R. a., Kain, T.R., 1990. Vegetation dynamics in impounded marshes along the Indian River Lagoon, Florida, USA. Environmental Management, 14(3), 397–409

Rodriguez, W. Feller, I.C., 2004. Mangrove landscape characterization and change in Twin Cays, Belize using aerial photography and IKONOS satellite data, Atoll Res. Bull. 513, 1-22

Silvestri, S., Oostdijk, M., Laanbroek , H.J., Rains, M., Verhoeven, J.T.A., Whigham, D.F., Using remote sensing to study mangroves spatial dynamics under increased nitrogen availability and lower salinity conditions, poster presented at: AGU Fall meeting, 19 December 2014, San Francisco

Stringer, C.E., Rains, M.C., Kruse, S., Whigham, D., 2010. Controls on Water Levels and Salinity in a Barrier Island Mangrove, Indian River Lagoon, Florida, Wetlands, 30: 725-734

Tomlinson, P.B., 1986. The Botany of Mangroves; Cambridge University Press: Melbourne, Australia

Updike, T., Comp, C., 2010. Radiometric Use of WorldView-2 Imagery Technical Note 1 WorldView-2 Instrument Description, 1–17.

Verhoeven, J. T. A, Laanbroek, H. J., Rains, M. C., Whigham, D. F. 2014. Effects of increased summer flooding on nitrogen dynamics in impounded mangroves. Journal of Environmental Management, 139: 217–226

Vogt, J., Skóra, A., Feller, I. C., Piou, C., Coldren, G., & Berger, U., 2012. Investigating the role of impoundment and forest structure on the resistance and resilience of mangrove forests to hurricanes. Aquatic Botany, 97(1), 24–29.

Whitlock, M., Schluter, D., 2009. The analysis of biological data, Roberts & Company publishers, Greenwood Village, USA

Wilhelm, W. W., Ruwe, K., Schlemmer, M. R., 2000. Comparison of three leaf area index meters in a corn canopy. Crop Science, 40, 1179–1183

Appendix 1. Average temperature and total precipitation, Fort Pierce 2000-2015

Meteo data retreived from: https://www.sercc.com/climateinfo/historical/historical_fl.html on July 10 2015

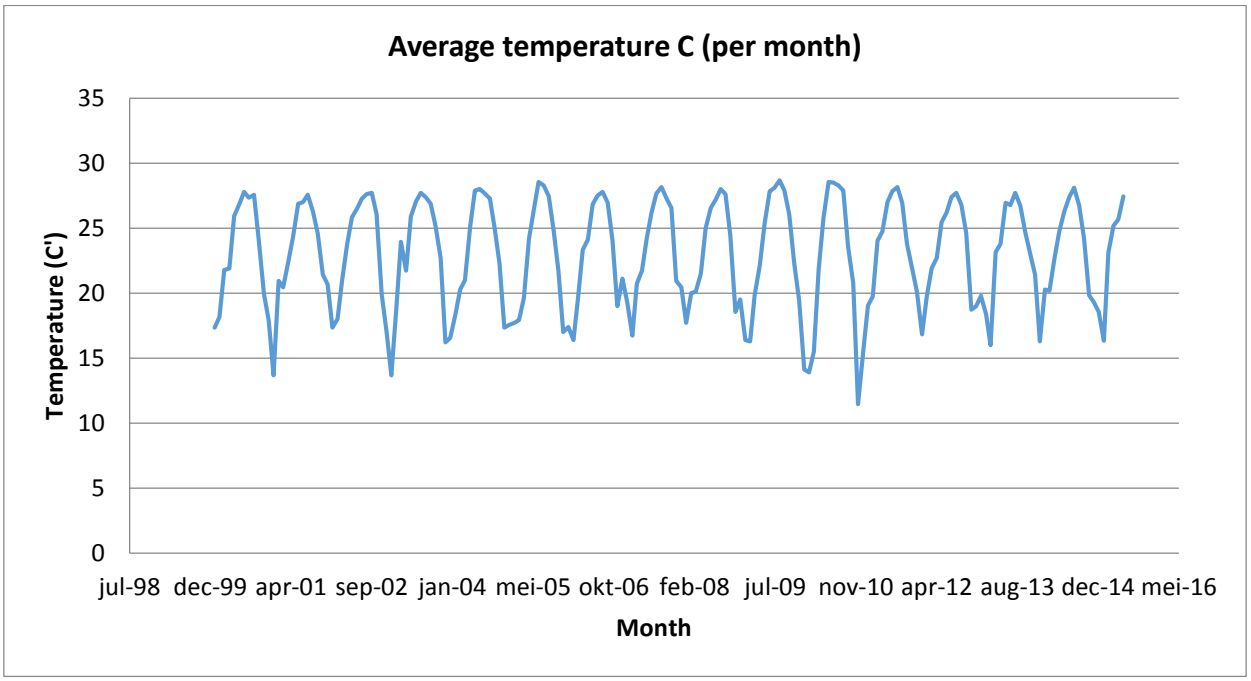

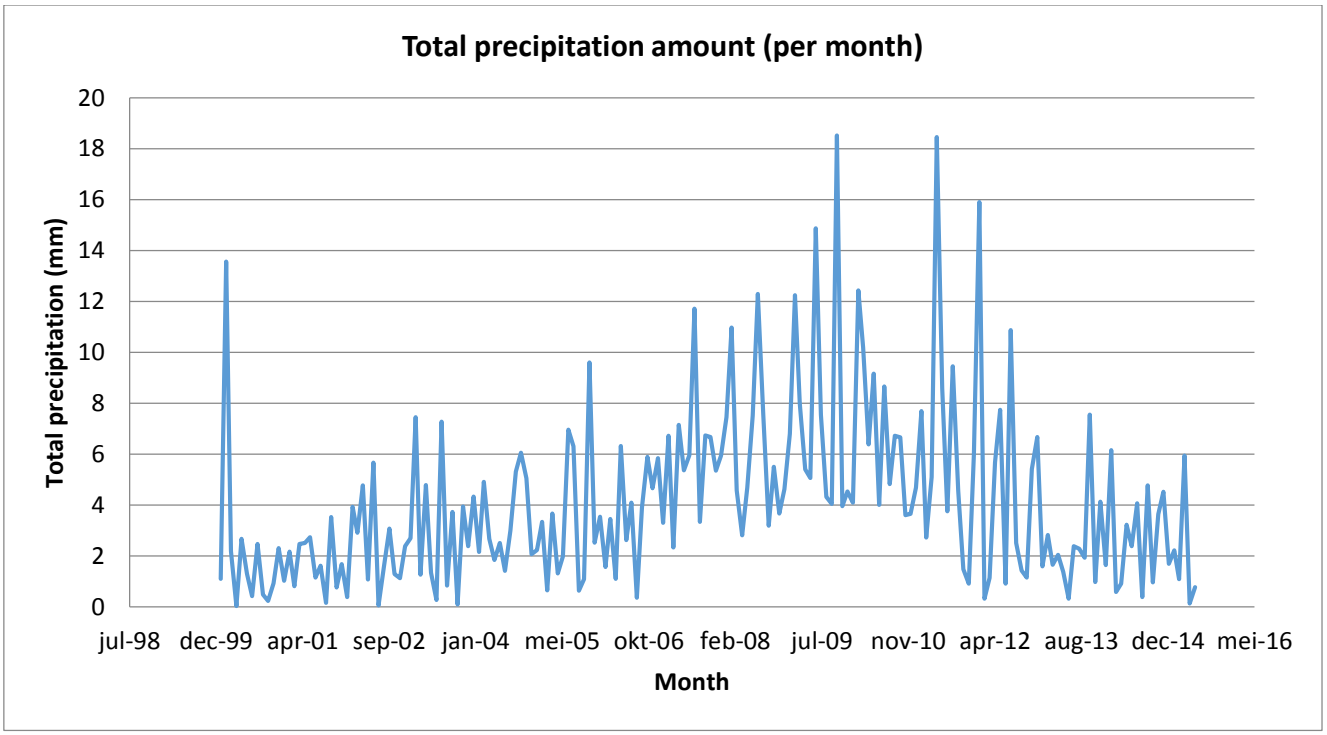

Appendix 2. Calibration lines used for the empirical line calibration of DM, UCX and WV2 panchromatic imagery

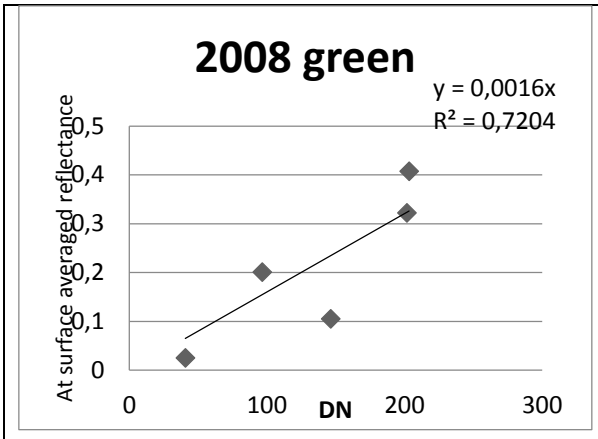

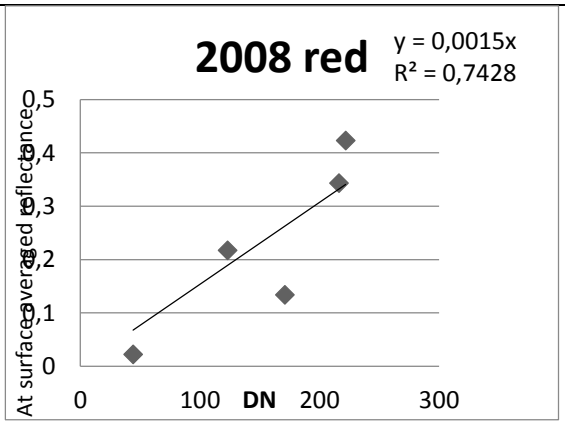

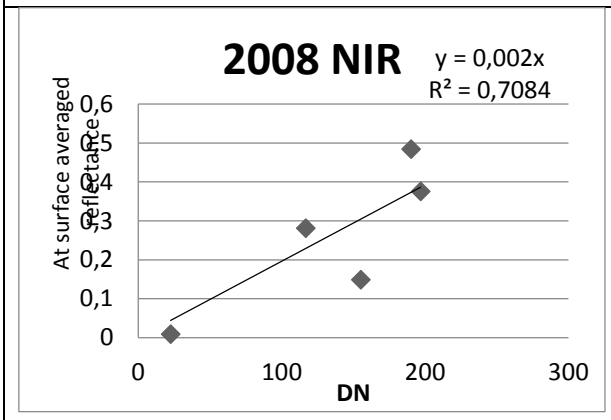

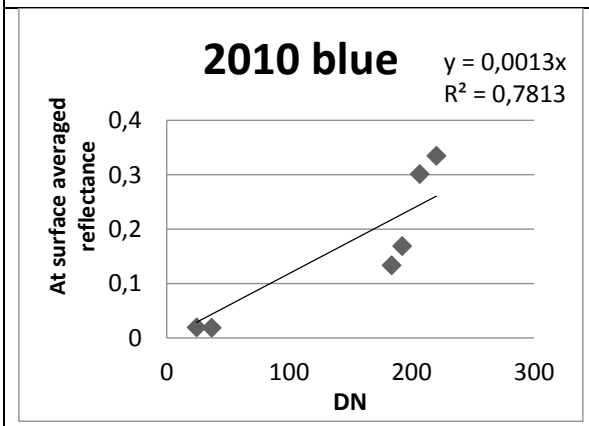

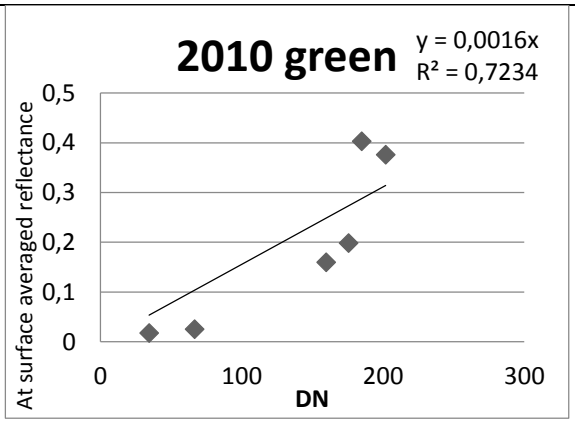

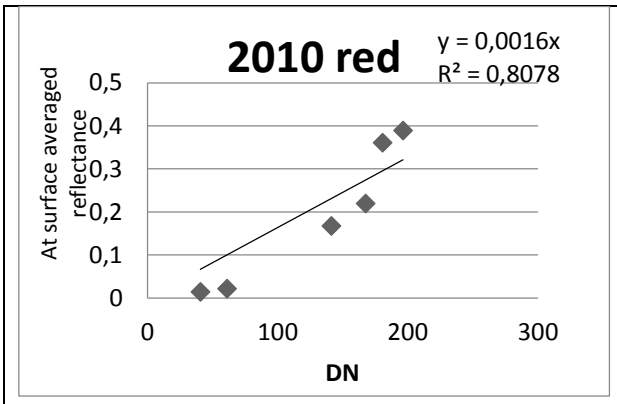
2010 red
y = 0,0016x
R² = 0,8078
At surface averaged reflectance
0,5
0,4
0,3
0,2
0,1
0
0
100
200
300
DN

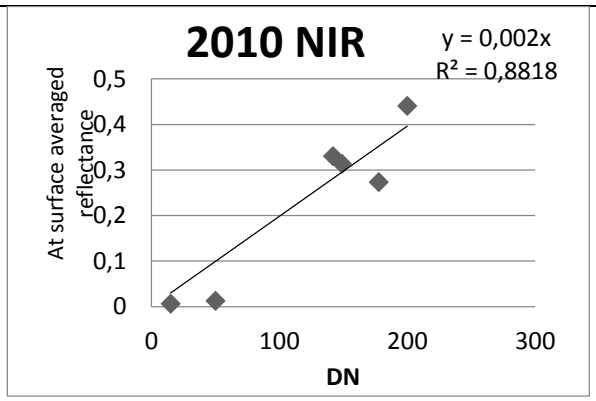
2010 NIR
y = 0,002x
R² = 0,8818
At surface averaged reflectance
0,5
0,4
0,3
0,2
0,1
0
0
100
200
300
DN

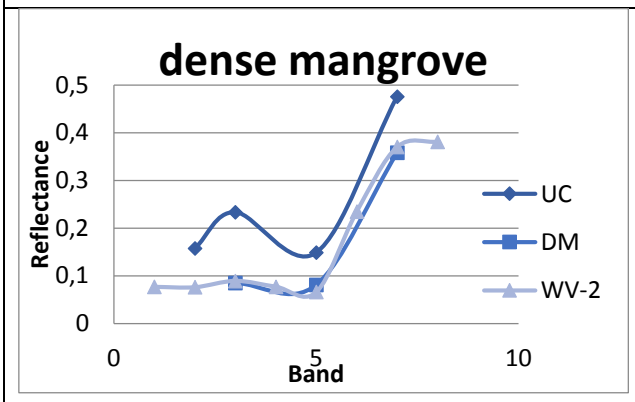
dense mangrove
Reflectance
0,5
0,4
0,3
0,2
0,1
0
0
5
10
Band
UC
DM
WV-2

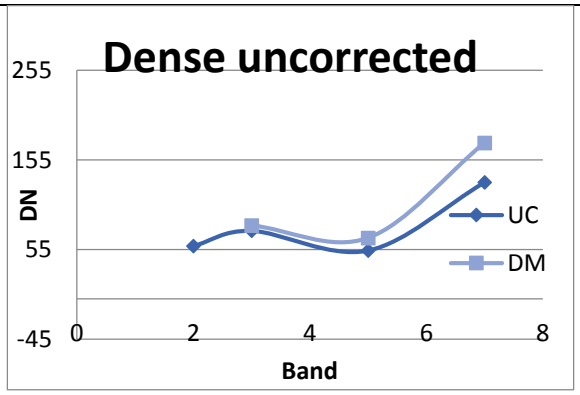
Dense uncorrected
DN
255
155
55
-45
0
2
4
6
8
Band
UC
DM

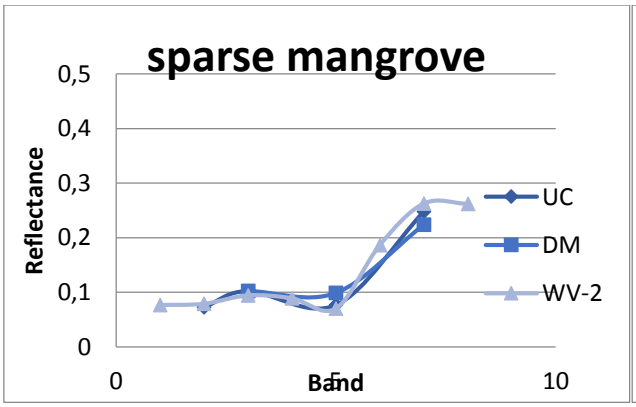
sparse mangrove
Reflectance
0,5
0,4
0,3
0,2
0,1
0
0
5
10
Band
UC
DM
WV-2

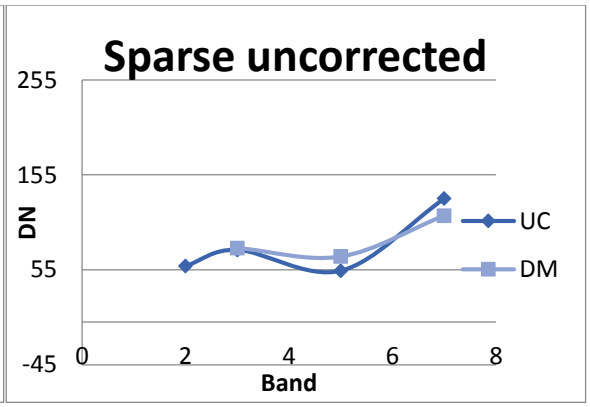
Sparse uncorrected
DN
255
155
55
-45
0
2
4
6
8
Band
UC
DM

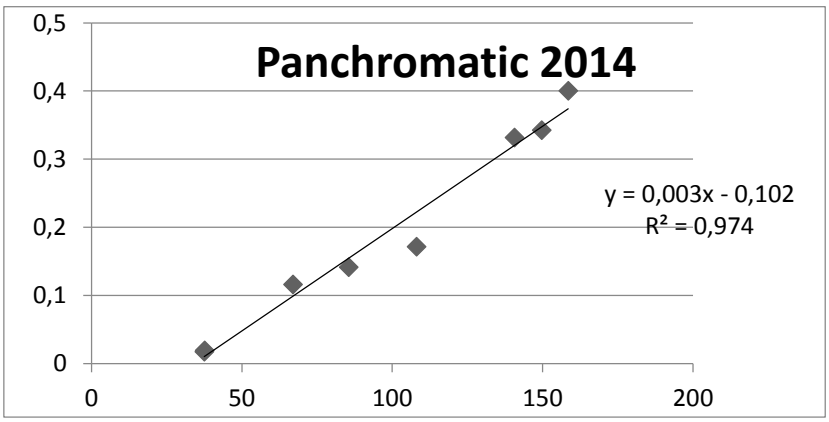
Panchromatic 2014
y = 0,003x - 0,102
R² = 0,974
0,5
0,4
0,3
0,2
0,1
0
0
50
100
150
200

Appendix 3. Error matrices of all classifications

Digital Mapping camera (2008)	Ground Truth	(Pixels)			
Class	soil	herbaceous	dwarf	sparse	dense
soil	675	38	6	0	0
herbaceous	25	178	65	0	0
dwarf	0	298	659	122	0
sparse	0	0	17	406	5
dense	0	0	0	141	762
Total	700	514	747	669	767

UltracamX (2010)

	Ground Truth	(Pixels)			
Class	soil	herbaceous	dwarf	Sparse	dense
soil	921	38	1	0	0
herbaceous	84	893	42	0	0
dwarf	0	111	921	313	0
sparse	0	0	95	630	103
dense	0	0	2	130	897
Total	1005	1042	1061	1073	1000

WV2 0.5m (2014)

	Ground Truth	(Pixels)			
Class	soil	herbaceous	dwarf	sparse	dense
soil	119	3	0	0	0
herbaceous	17	321	39	0	0
dwarf	8	103	282	76	0
sparse	0	0	61	464	19
dense	0	0	0	47	550
Total	144	427	382	587	569

WV2 2m (2014)

	Ground Truth	(Pixels)			
Class	soil	herbaceous	dwarf	sparse	dense
soil	22	0	0	0	0
herbaceous	4	22	5	1	0
dwarf	0	6	27	13	0
sparse	0	0	5	55	1
dense	0	0	0	17	129
Total	26	28	37	86	130

WV2 0.5m Maximum likelihood

Class	soil	herbaceous	dwarf	sparse	dense
Unclassified	36	8	0	0	0
soil	86	16	3	2	0
herbaceous	23	280	31	0	0
dwarf	0	124	293	81	0
sparse	0	0	54	414	4
dense	0	0	1	90	565
Total	145	428	382	587	569

Appendix 4. Results for t-tests and Mann-Whiney U tests performed for all sites

	T-tests before-after										
Dwarf 2008-2010		Mean	Std.Dv.	N	Diff.	Std.Dv.	t	df	p	Confidence	Confidence
	2008 soil	**73,23764**	**16,11295**								
	2010 soil	**31,34350**	**30,81932**	**5**	**41,8941**	**21,78974**	**4,29919**	**4**	**0,012654**	**14,8386**	**68,9497**
	2008 herb	23,26458	13,55608								
	2010 herb	35,19066	19,97494	5	-11,926	17,92454	-1,4877	4	0,211029	-34,1823	10,3302
	2008 dwarf	**3,42932**	**3,37897**								
	2010 dwarf	**28,12782**	**16,30185**	**5**	**-24,698**	**15,41918**	**-3,5817**	**4**	**0,023132**	**-43,8439**	**-5,5531**
	2008 sparse	0,00000	0,00000								
	2010 sparse	4,06556	4,01604	5	-4,0656	4,01604	-2,2636	4	0,086333	-9,0521	0,9210
	2008 dense	0,00000	0,00000								
	2010 dense	1,11740	1,80656	5	-1,1174	1,80656	-1,3830	4	0,238835	-3,3605	1,1257
	2008 soil	0,00000	0,00000								
sparse 2008-2010	2010 soil	0,95482	1,83926	5	-0,9548	1,83926	-1,1608	4	0,310273	-3,239	1,32892
	2008 herb	0,28493	0,24676								
	2010 herb	5,71783	6,33807	3	-5,4329	6,16228	-1,5270	2	0,266308	-20,741	9,87505
	2008 dwarf	27,75738	26,05339								
	2010 dwarf	30,05282	19,29030	5	-2,2954	24,18123	-0,2122	4	0,842280	-32,320	27,72952
	2008 sparse	52,66102	22,30115								
	2010 sparse	24,90504	13,27015	5	27,7560	32,70739	1,89756	4	0,130606	-12,856	68,36756
	2008 dense	18,87112	23,50393								
	2010 dense	33,82266	33,38848	5	-14,951	24,90294	-1,3425	4	0,250555	-45,873	15,96954
dense 2008-2010	2008 herb	0,25946	0,58017								
	2010 herb	1,33946	2,13338	5	-1,0800	2,21177	-1,0918	4	0,336248	-3,8263	1,6663
	2008 dwarf	17,51572	17,37421								

	2010 dwarf	16,32008	15,34356	5	1,1956	10,71739	0,24946	4	0,815293	-12,1118	14,5030
	2008 sparse	38,02256	5,91729								
	2010 sparse	27,26862	16,51873	5	10,7539	12,34757	1,94747	4	0,123315	-4,5776	26,0855
	2008 dense	44,20224	23,42884								
	2010 dense	54,98484	31,42817	5	-10,782	17,67545	-1,3640	4	0,244255	-32,7296	11,1644

T-tests 23 vs.24 2010												
		Mean	Mean	t-value	df	p	Valid N	Valid N	Std.Dev.	Std.Dev.	F-ratio	p
Dwarf 23 &24	herb.	35,19066	32,01276	0,25616	8	0,804294	5	5	19,97494	19,24981	1,076758	0,944585
	dwarf	**28,12782**	**58,92212**	**-2,99540**	**8**	**0,017192**	**5**	**5**	**16,30185**	**16,20788**	**1,011629**	**0,991328**
Sparse 23 &24	dwarf	**30,05282**	**60,77836**	**-2,34432**	**8**	**0,047097**	**5**	**5**	**19,29030**	**22,06280**	**1,308106**	**0,800956**
	sparse	24,90504	18,46200	0,80277	8	0,445301	5	5	13,27015	12,08257	1,206237	0,860190
Dense	herb.	1,33946	3,81752	-1,69007	8	0,129484	5	5	2,13338	2,48960	1,361830	0,771999
	dwarf	54,98484	40,50864	0,80204	8	0,445701	5	5	31,42817	25,32114	1,540535	0,685670
	sparse	27,26862	27,81004	-0,06869	8	0,946925	5	5	16,51873	6,14788	7,219414	0,081608
	dense	16,32008	25,58900	-0,98676	8	0,352661	5	5	15,34356	14,34384	1,144250	0,899243

Mann-Whitney 23 vs. 24 2010											
Dwarf 23 &24		Rank Sum	Rank Sum	U	Z	p-value	Z	p-value	Valid N	Valid N	2*1sided
	soil	37,00000	18,00000	3,00000	1,88004	0,060104	1,88004	0,060104	5	5	0,055556
	sparse	31,00000	24,00000	9,00000	0,62668	0,530870	0,62668	0,530870	5	5	0,547619
	dense	31,00000	24,00000	9,00000	0,62668	0,530870	0,63442	0,525809	5	5	0,547619
Sparse 23 &24	soil	26,50000	28,50000	11,50000	-0,10445	0,916815	-0,10476	0,916563	5	5	0,841270
	herb.	32,00000	23,00000	8,00000	0,83557	0,403396	0,83557	0,403396	5	5	0,420635
	dense	34,00000	21,00000	6,00000	1,25336	0,210076	1,25336	0,210076	5	5	0,222222

	T-tests Rate of change sparse (RIM vs. Non imp)											
		Mean - RIM	Mean - non imp	t-value	df	p	Valid N - RIM	Valid N - non imp	Std.Dev. - RIM	Std.Dev. - non imp	F-ratio - Variances	p-variances
Sparse	sparse	-27,7560	-10,6919	-1,15178	8	0,282669	5	5	32,70739	5,264684	38,59643	0,003762
Dense	dwarf	-1,1956	1,2629	-0,4858	8	0,640138	5	5	10,71739	3,63333	8,7	0,059374
	dense	10,7826	-11,6871	2,10634	8	0,068260	5	5	17,67545	16,01778	1,22	0,853232

	Mann-Whitney Rate of change sparse (RIM vs. Non imp)										
		Rank Sum	Rank Sum	U	Z	p-value	Z	p-value	Valid N	Valid N	2*1sided
Sparse RIM & non-imp.	dwarf soil	18,00000	37,00000	3,00000	-1,88004	0,060104	-1,89154	0,058554	5	5	0,055556
	herb.	25,00000	30,00000	10,00000	-0,41779	0,676104	-0,42034	0,674236	5	5	0,690476
	dwarf	33,00000	22,00000	7,00000	1,04447	0,296271	1,05085	0,293326	5	5	0,309524
	dense	27,00000	28,00000	12,00000	0,00000	1,000000	0,00000	1,000000	5	5	1,000000
Dense RIM & non-imp.	herb.	33,00000	22,00000	7,000000	1,04447	0,296271	1,17670	0,239317	5	5	0,309524
	sparse	18,00000	37,00000	3,000000	-1,88004	0,060104	-1,88004	0,060104	5	5	0,055556